

# Materials Science and Materials Chemistry for Large Scale Electrochemical Energy Storage: From Transportation to Electrical Grid

Jun Liu,\* Ji-Guang Zhang, Zhenguo Yang, John P. Lemmon, Carl Imhoff, Gordon L. Graff, Liyu Li, Jianzhi Hu, Chongmin Wang, Jie Xiao, Gordon Xia, Vilayanur V. Viswanathan, Suresh Baskaran, Vincent Sprenkle, Xiaolin Li, Yuyan Shao, and Birgit Schwenzer

Large-scale electrical energy storage has become more important than ever for reducing fossil energy consumption in transportation and for the widespread deployment of intermittent renewable energy in electric grid. However, significant challenges exist for its applications. Here, the status and challenges are reviewed from the perspective of materials science and materials chemistry in electrochemical energy storage technologies, such as Li-ion batteries, sodium (sulfur and metal halide) batteries, Pb-acid battery, redox flow batteries, and supercapacitors. Perspectives and approaches are introduced for emerging battery designs and new chemistry combinations to reduce the cost of energy storage devices.

## 1. Introduction

Large-scale electrical energy storage has received worldwide attention for reducing fossil energy consumption in automobiles (transportation application) and for the widespread use of intermittent renewable energy in the modern electrical grid (stationary application). For transportation, the goal for the US Department of Energy (DOE) and the automobile industry is to develop a battery with an energy density of 300 Wh/L and 250 Wh/kg with a cost of \$125/kWh in order to enable the 300-mile range mid-sized sedan. For energy applications on the electrical grid, the cost needs to be even lower, in the low \$100/kWh range to achieve 20% wind penetration on the grid by 2030. Great effort has been made to identify and address the scientific challenges for high performance energy storage technologies for the transportation sector, in particular for plug-in hybrid electrical and fully electrical vehicles (PHEVs and

EVs), while fundamental chemistry and materials problems involved in stationary energy storage systems have received less attention in the materials community.<sup>[1]</sup>

The performance requirements for the transportation and stationary storage areas can be quite different. The energy density is critical for the former, and low cost and scalability are more important in the later. As a result, Li-ion batteries have been the main focus for auto application, but many other technologies are considered for stationary applications. In addition, batteries for the auto industry involve a much narrower charge/discharge time window of a

few seconds, while for large-scale energy storage in backup systems for power grids the response time (or discharge duration) ranges from seconds to many hours or longer and the later must provide a much broader power/energy range.<sup>[1–3]</sup> Nevertheless there are similar scientific challenges involved the fundamental chemistry and properties of the electrode and electrolyte materials. Therefore, this article aims to discuss important cross-cutting, fundamental materials science and materials chemistry challenges that are applicable to a range of electrochemical energy storage technologies encountered, starting with a brief overview of the general technologies in both transporting and stationary applications and followed by more in-depth discussion of specific materials and chemistry problems. While it is not possible to discuss all topics in this broad range of technologies or review all publications in this field, this paper will attempt to 1) provide an overview of current device and technologies; 2) highlight the critical materials by discussing the underlying technology, their advantages and problems using specific examples, and results from recent efforts to reduce the cost and improve the performance of electrochemical energy storage devices; and 3) introduce perspectives and approaches for emerging battery designs and new chemistry combinations to reduce the cost of energy storage devices.

In the last few years, public and private sectors have made significant investments in energy storage media for PHEVs and fully EVs. In these applications, Li-ion batteries are attractive because high energy/power densities are critical based on the

Dr. J. Liu, Dr. J.-G. Zhang, Dr. Z. Yang, Dr. J. P. Lemmon, Dr. C. Imhoff, Dr. G. L. Graff, L. Li, J. Hu, C. Wang, J. Xiao, G. Xia, V. V. Viswanathan, S. Baskaran, V. Sprenkle, X. Li, Y. Shao, B. Schwenzer  
Pacific Northwest National Laboratory  
Richland, WA, 99352, USA  
E-mail: Jun.Liu@pnnl.gov



DOI: 10.1002/adfm.201200690

constraints on weight and volume.<sup>[4–6]</sup> Other emerging, high-capacity rechargeable Li batteries, such as Li-S batteries<sup>[7–9]</sup> and Li-air batteries,<sup>[9–15]</sup> still have poor cycle life and high cost, but they are viewed as candidates that can potentially meet DOE's long-term performance goals for energy storage in transportation. The stationary energy storage market, on the other hand, includes applications that range from kW to MW and GW systems (Figure 1a) and it is very difficult to identify a single technology or a single target for different applications. The technology can be deployed for single customer users, communities, or on the generation sites. The function could include reducing the variability of renewable generators, particularly wind and solar, easing their ramp rates, and moving energy generated during off-peak times to meet on-peak needs.<sup>[16,17]</sup> Energy storage can also raise the duty factor of the grid, decrease the need to upgrade systems to meet growing peak demands, provide emissionless regulation, and increase power quality. The performance and cost targets depend on the specific applications as well as the location and the local economy and energy infrastructure (Figure 1b). The difference in life cycle cost (capital cost/number of charge-discharge cycles/round trip efficiency) is even greater, considering that the devices for stationary storage must maintain performance and safety standards for more than 10 years.

Some technologies such as Li-ion batteries developed for the transportation industry could also be applicable for power grid enhancement. Small-scale energy storage devices will be suitable and necessary for power management closer to the end user or for distributed storage in grid applications, while other

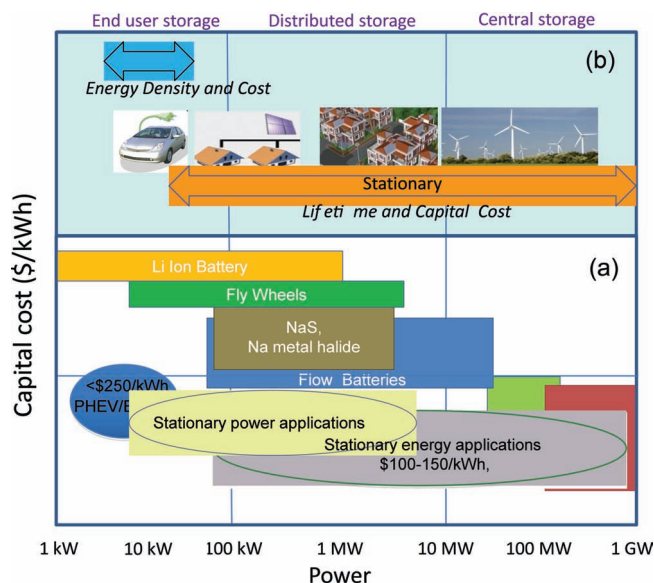


**Figure 1.** Comparison of cost and performance requirements for transportation and stationary energy storage (schematic). a) The stationary applications cover a much wider range of applications and a wider range of storage (discharge) times and power/energy scales than PHEVs.<sup>[2]</sup> PHEVs require tens of kW power and need a response (discharge) time over tens of seconds. b) Different applications and technologies are being considered for energy storage and the cost comparisons. The cost of PHEV storage can be higher than stationary power applications, which can be higher than the energy applications in stationary storage.



**Dr. Jun Liu** is a Laboratory Fellow at the Pacific Northwest National Laboratory and leader for the Transformational Materials Science Initiative. Dr. Liu's main research interest includes synthesis of functional nanomaterials for energy storage, catalysis, environmental separation and health care.

large-scale energy storage technologies are needed to allow for optimum use of existing and new energy assets, improve the reliability of the electricity supply, and support the integration of large-capacity, intermittent renewable energy resources.<sup>[16,17]</sup>

A recent study suggested that to meet the target of 20% renewable wind energy production by 2030 in the United States, tens of GW of power storage capacity must be needed for balancing requirements (matching the demand and supply on the grid) introduced by the variability of intermittent resources.<sup>[18]</sup> Other estimates are as high as a few hundred GWh of energy storage necessary to accommodate up to 20% of the renewable portfolio standard for storing and moving energy through the renewable cycles.<sup>[19–21]</sup> Considering the wide range of storage applications from fast (up to 10 s) frequency regulation to slow load shifting over hours or longer, understanding these important issues, such as how much energy storage is required for a particular applications, what the performance requirements will be, what technologies should be used, and what the potential cost constraints are, are all very important questions that need to be answered. Furthermore, the benefits and economic viability of grid storage are still being vigorously debated, and the cost and long-term performance of storage devices with all ranges of storage capacity also need to be significantly improved to make them economically more competitive.<sup>[22]</sup>

## 2. Storage Technologies

### 2.1. Overview

A wide range of technologies are currently being evaluated for energy storage including 1) supercapacitors,<sup>[23,24]</sup> Li-ion batteries,<sup>[25]</sup> and Pb-acid batteries for both portable and stationary applications; 2) flywheels<sup>[26,27]</sup> and supercapacitors<sup>[23,24]</sup> for auto application and power management and regulation on grid (storage to ensure the continuity, quality, and desired frequency of the electricity); and 3) Na-S-based<sup>[28]</sup> and redox flow batteries<sup>[29]</sup> for MW-level energy management (storage to solve the timing problem of energy generation and consumption), compressed air, and pumped hydro for large-scale applications beyond MW levels. It is also unlikely that any individual technology can meet all the requirements to store energy for

**Table 1.** Main applications, advantages, and limitations of different energy storage technologies.

Technology	Main Application	Advantages	Limitations
Li-ion battery	transportation; portable electronics; power application on grid is being investigated	near 100% efficiency; high energy density; high power	high capital cost (~\$700/kWh); safety and reliability problems due to heat management issues; small temperature range of operation
Pb-acid battery	current automobile and electrical bikes, buses; backup power; industrial applications	least expensive in terms of capital cost (\$/kWh)	short cycle life; high maintenance; high lifecycle cost (\$/kWh/cycle); low specific energy due to insufficient materials utilization
Na-S and Na-metal halide battery	research targets grid-scale storage	efficiencies up to 90%; energy densities comparable to current Li-ion batteries	operating range of 300–350 °C; safety and durability concerns (e.g., fire in case of membrane and package failure); high production cost; current specifications (weight and size) limit potential applications
Redox flow battery (RFB)	grid-scale storage	MW storage system; power and energy capacity are independently tunable and adjustable; potential long cycle life	high capital cost; long term durability not proven; capacity loss issues like self-discharge over time; electrolyte stability at different temperatures; stack design and grid integration challenges

different scales and applications. Electrochemical energy storage is currently the most versatile technology because of its flexibility to cover wide energy and time domains. Advantages and limitations of some important technologies are listed in Table 1.

The details of all different technologies will be discussed here and in other articles, but to simplify the discussion, we use Table 2 and three examples to illustrate the fundamental materials and chemistry issues.

In addition to batteries and supercapacitors, electrochemical capacitors are also widely investigated and are useful for high power applications (for example, ultrafast charge under 30 miles/min) in automobiles and frequency regulations on grid. Due to limited space, only a brief summary is provided here. There are two types of electrochemical capacitors, electrical double layer capacitor and the pseudocapacitors. High surface area carbon is the leading electrode material.<sup>[24,51]</sup> A wide range of high surface area carbon materials have been investigated, including activated carbon, multi- and single-walled carbon nanotubes, and graphene. The capacitance typically ranges from 40 to 140 F/g for activated carbon<sup>[24]</sup> and 15 to 135 F/g for carbon nanotubes.<sup>[52,53]</sup> Currently, the best available result from commercial products is about 130 F/g (Maxwell's BoostCap). Pseudo electrochemical capacitance involves voltage-dependent Faradaic reactions between the electrode and the electrolyte, either in the form of surface adsorption/desorption of ions, redox reactions with the electrolyte, or doping/undoping of the electrode materials. Hydrous RuO<sub>2</sub> is an excellent, but expensive electrode material.<sup>[54–57]</sup> Other metal oxides,<sup>[58]</sup> nitrides,<sup>[59–62]</sup> and doped conducting polymers are also under investigation.<sup>[63–65]</sup>

Currently, Li-ion batteries are still too expensive (above \$700/kWh) and the energy density is not sufficient for long range EV. For stationary application, the cost is over \$3000/kWh for power applications and over \$500/kWh for energy applications. Some current technologies, including Li-ion batteries,<sup>[25]</sup> flywheels, supercapacitors,<sup>[23,24]</sup> and even Na-S batteries<sup>[28]</sup> may have a potential for initial market penetration for power-balancing requirements,<sup>[20]</sup> but significant breakthroughs are needed to reduce the cost of large-scale energy storage by a factor of 3 to

5 times, to a \$100 to 150/kWh range, for large-scale stationary applications. In addition, efficiency, life cycle, and safety also need to be significantly improved (Table 1). A better fundamental understanding of the complex chemical and material processes involved in the current and future energy storage systems is needed to predict the cost and performance. Revolutionary designs, concepts, and architectures are desired to reduce the system and maintenance costs. There is also a great need to improve the structures and properties of materials and components to enhance efficiency, reliability, safety, and life span. In the long run, ultralow cost and environmentally benign storage technologies are needed. These novel approaches have to be based on novel, groundbreaking energy storage mechanisms that are environmentally friendly and do not depend on supply-limited materials and chemicals. Mathematical tools and methodologies must also be developed to predict and analyze the economics of specific technologies for different scales/different applications and for guiding smart grid integration.

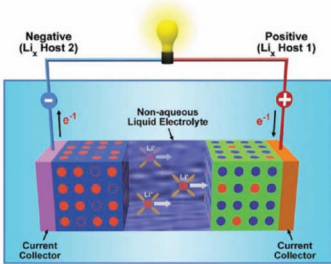
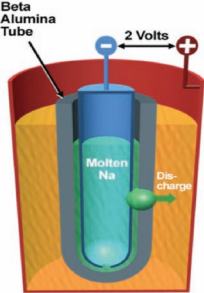
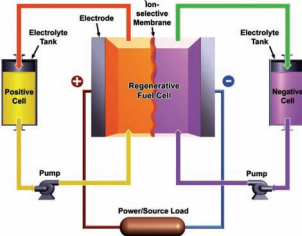
## 2.2. Materials and Components

### 2.2.1. Electrode Materials

Great efforts and tremendous progress have been made in the design and synthesis of nanostructured electrode materials to improve the performance of Li-ion batteries.<sup>[66]</sup> Currently, the main focuses are concentrated on two areas: identifying novel redox couple cathode materials that can have higher theoretical capacity and higher energy density than known ones such as LiFePO<sub>4</sub> and exploring new methods to improve the stability of high capacity anode materials, in particularly alloy mechanism based Sn and Si anodes.

Conventional cathode materials (such as LiCoO<sub>2</sub>, LiMn<sub>2</sub>O<sub>4</sub>, and LiFePO<sub>4</sub>) usually have 140–170 mAh/g capacity, while conventional graphite-based anode exhibits a theoretical capacity of ≈372 mAh/g. This means that the weight of the cathode material is often more than twice as heavy as that of anode. In the future, the energy density will be further increased and this imbalance

**Table 2.** Brief descriptions of how the different electrochemical storage devices work.

Li-ion Batteries	
	<p>Li-ion batteries store electrical energy in electrodes that are made of Li-intercalation (or insertion) compounds. During charge and discharge, <math>\text{Li}^+</math> ions transfer across a liquid organic electrolyte between one host structure and the other, with concomitant oxidation and reduction processes occurring at the two electrodes. Figure reproduced with permission.<sup>[253]</sup> Copyright 2010, Springer.</p> <p>Key materials problems: cathode capacity is limited; high capacity anode is not very reversible; need to develop safer electrolytes.</p>
Na-S or Na-metal halide Batteries	
	<p>In Na-S<sup>28</sup> and Na-MH batteries,<sup>[30–36]</sup> reversible charge and discharge occurs via a <math>\text{Na}^+</math> ion conducting, solid state <math>\beta''\text{-Al}_2\text{O}_3</math> membrane that is stabilized with <math>\text{Li}_2\text{O}</math> or <math>\text{MgO}</math>.<sup>[37,38]</sup> To achieve a satisfactory ionic conductivity (<math>\sigma = 0.3 \text{ s}^{-1} \text{ cm}</math>, <math>300^\circ\text{C}</math>, for <math>\beta''\text{-Al}_2\text{O}_3</math>), these batteries operate at <math>\approx 300</math> to <math>350^\circ\text{C}</math> using liquid sodium as anodes. The cathode is composed of molten <math>\text{S}/\text{Na}_2\text{S}_x</math> that is added to porous graphite felts to improve its electron conductivity. This overall electrochemical reaction gives a standard voltage (1.78 to 2.08 V) for <math>x = 3</math>–5. Currently, most of these batteries use a tubular design (<math>\beta''\text{-Al}_2\text{O}_3</math> tube). One major advantage of the high-temperature Na battery is its high energy efficiency (up to 90%), due to in part to its nearly 100% coulombic efficiency. In addition, the molten electrodes in the battery ensure a high current density and a quick response to the changes of power conditions, both of which are important to utility or stationary applications. As an alternate to the molten <math>\text{S}/\text{Na}_2\text{S}_x</math> cathode, porous <math>\text{Ni}/\text{NiCl}_2</math> structures impregnated with molten <math>\text{NaAlCl}_4</math> are used in Na-MH batteries that offer several advantages including 1) improved safety in the event of a BASE membrane failure; 2) short-circuit mechanism in the cell results in a closed configuration that minimizes series-wired battery pack losses; and 3) cells are built in the discharged state that avoids the handling of metal sodium and results in significant reductions in manufacture cost and safety.</p> <p>Key materials problems: membranes and electrolytes are only conductive at high temperatures; corrosive electrolytes; packaging and sealing are difficult. (Figure reproduced with permission.<sup>[38]</sup> Copyright 2010, Elsevier.)</p>
Redox Flow Batteries (RFBs)	
	<p>RFBs store electrical energy in two soluble redox couples contained in external electrolyte tanks.<sup>[29,39–41]</sup> Aqueous liquid electrolyte is pumped from the storage tanks to flow through electrodes where chemical energy is converted to electrical energy (discharge) or vice versa (charge). The electrolytes are separated by a proton membrane or a separator. The power and energy capacity can be designed separately. The power of the system is determined by the size of the electrodes and the number of cells in a stack, whereas the energy storage capacity is determined by the concentration and volume of the electrolyte. Many redox couples have been investigated,<sup>[42,43]</sup> including (<math>\text{Fe}^{2+}/\text{Fe}^{3+} \parallel \text{Cr}^{2+}/\text{Cr}^{3+}</math>),<sup>[42,43]</sup> <math>\text{Ce}^{4+}/\text{Ce}^{3+}</math> vs. <math>\text{V}^{2+}/\text{V}^{3+}</math>,<sup>[44]</sup> <math>\text{Fe}^{3+}/\text{Fe}^{2+}</math> vs. <math>\text{Br}_2/\text{Br}^-</math>,<sup>[45]</sup> <math>\text{Mn}^{2+}/\text{Mn}^{3+}</math> vs. <math>\text{Br}_2/\text{Br}^-</math>,<sup>[46]</sup> <math>\text{Fe}^{3+}/\text{Fe}^{2+}</math> vs. <math>\text{Ti}^{2+}/\text{Ti}^{4+}</math>, polysulfide-bromide (PSB),<sup>[47,48]</sup> zinc-bromide batteries (ZBB),<sup>[49]</sup> and <math>\text{V}^{2+}/\text{V}^{3+}</math> vs. <math>\text{V}^{4+}/\text{V}^{5+}</math> (VRBs).<sup>[39,50]</sup> All-vanadium redox batteries (VRBs) have attracted the most attention because they use vanadium ions in both the anolyte and catholyte. This mitigates the cross-contamination of active species through the membrane. The overall electrochemical reaction in RFBs gives a cell voltage of 1.26 V at <math>25^\circ\text{C}</math> and unit activities (i.e., standard voltage).</p> <p>Key materials problems: low solubility and energy density; cross-over in membranes; long term stability in electrolytes. (Figure reproduced with permission.<sup>[19]</sup>)</p>

between cathodes and anodes may become more serious. On the other hand, the cost of the cathode often is more than 40% of that in Li-ion batteries. Therefore, improvement in the performance and cost of cathode materials is a very efficient way to improve the performance and cost of full Li-ion batteries.<sup>[67,68]</sup>

The olivine-structured  $\text{LiFePO}_4$  has been successfully developed.<sup>[69–72]</sup> The conductivity has been greatly increased by reducing the particle sizes or by applying Na electrically conductive coatings.<sup>[73,74]</sup> In the past few years, other  $\text{LiMPO}_4$  (M = Mn, Co, and Ni) structures, in particular  $\text{LiMnPO}_4$  with a higher theoretical energy density, (701 Wh/kg) 171 mAh/g  $\times$  4.1 V, due to higher potential than that of  $\text{LiFePO}_4$ , (586 Wh/kg) 170 mAh/g  $\times$  3.45 V.<sup>[75–77]</sup> However, the ionic conductivity and the electronic conductivity of  $\text{LiMnPO}_4$  ( $<10^{-10} \text{ Scm}^{-1}$ ) is much lower than that of  $\text{LiFePO}_4$  ( $1.8 \times 10^{-9} \text{ Scm}^{-1}$  at  $25^\circ\text{C}$ ),

making it difficult to obtain good electrochemical activity.<sup>[78,79]</sup> Many other problems, such as the intrinsic instability of the structure, also causes problems on the capacity and reliability for the material.<sup>[80,81]</sup>

Another very promising cathode for the long range electrical applications is a layered composite cathode represented by  $x\text{Li}_2\text{MnO}_3 \cdot (1-x)\text{LiNi}_{0.45}\text{Mn}_{0.3}\text{Co}_{0.25}\text{O}_2$ .<sup>[82]</sup> The highest capacity reported for layered composites  $x\text{Li}_2\text{MnO}_3 \cdot (1-x)\text{LiMO}_2$  (M = Mn, Ni, Co) is about 200 mAh/g at 1C rate. However, many issues that need to be addressed, such as low initial efficiency, poor rate capability, and huge voltage profile change due to slow transformation into spinel phase leading to serious capacity loss. The reason for the voltage drop after cycling is still unclear and more fundamental studies should be deployed to address the challenges.



Other high voltage cathode material such as  $\text{LiNi}_{0.5}\text{Mn}_{1.5}\text{O}_4$  spinel<sup>[83,84]</sup> has also been investigated.  $\text{LiNi}_{0.5}\text{Mn}_{1.5}\text{O}_4$  spinel has a theoretical capacity of 146 mAh/g. The two valence states of Ni ( $\text{Ni}^{3+}$  and  $\text{Ni}^{4+}$ ) becomes accessible at 4.7 V to 4.8 V (vs.  $\text{Li/Li}^+$ ) because those redox couples are pinned at the top of O-2p bands. Accordingly, the energy density of  $\text{LiNi}_{0.5}\text{Mn}_{1.5}\text{O}_4$  (650 Wh/kg) is 20% and 30% higher than that of conventional  $\text{LiCoO}_2$  and  $\text{LiFePO}_4$  cathodes, respectively. Retaining high capacity at a high power rate is especially important for PHEV applications. Therefore, both  $\text{LiNi}_{0.5}\text{Mn}_{1.5}\text{O}_4$  and  $x\text{Li}_2\text{MnO}_3 \cdot (1-x)\text{LiMO}_2$  ( $\text{M} = \text{Mn, Ni, Co}$ ) composite are considered as very promising cathode materials for high energy Li-ion batteries.

For the anode in Li-ion batteries, Si is a promising candidate because of its high theoretical capacity and low discharge potential.<sup>[85,86]</sup> However, the large volume change of Si during cycling leads to a fast capacity fading. Significant research effort has been made to overcome this barrier.<sup>[87–115]</sup> Nanostructured Si such as nanoparticles,<sup>[87]</sup> nanowires,<sup>[88,89]</sup> and nanotubes<sup>[90,91]</sup> have been studied to reduce the structural degradation and volume. Progress has also been made in developing new binders,<sup>[92–94]</sup> electrolyte additives,<sup>[95,96]</sup> and conductive additives such as graphite,<sup>[97]</sup> amorphous carbon,<sup>[98–100]</sup> carbon nanotubes,<sup>[101]</sup> carbon nanofibers,<sup>[86,102,115]</sup> graphene sheets,<sup>[103–105,116]</sup> and metals.<sup>[106–109]</sup> Hollow Si nanospheres, porous Si, and porous Si-C composites have been shown to greatly improve the performance.<sup>[110–114]</sup> Pre-existing pores in Si-based materials provide the void space needed to accommodate volume changes (i.e., expansion/shrinkage) and also good access for the fast transport of Li ions. Stable cycling with initial capacities close to the theoretical value can be obtained.<sup>[111,114]</sup>

Although the volume expansion is considered the most significant problem, the detailed failure mechanisms are not well understood. Currently, more stable, high capacity results have mostly obtained from very thin film type of materials. Thicker electrodes obtained from more realistic scalable methods have poorer performance. In addition, the results are affected by many other factors, such as impurities in the electrolytes, additives in the form of binders, conducting carbon, etc. Rational explanation of such complex effects is still limited.

There are at least three mechanisms to cause the failure of the Si anode: mechanical instability caused by cracking and pulverization of the Si material, loss of electrical contacts among the Si particles and between the active materials and the substrate, and electrochemical instability caused by the breakdown of the solid

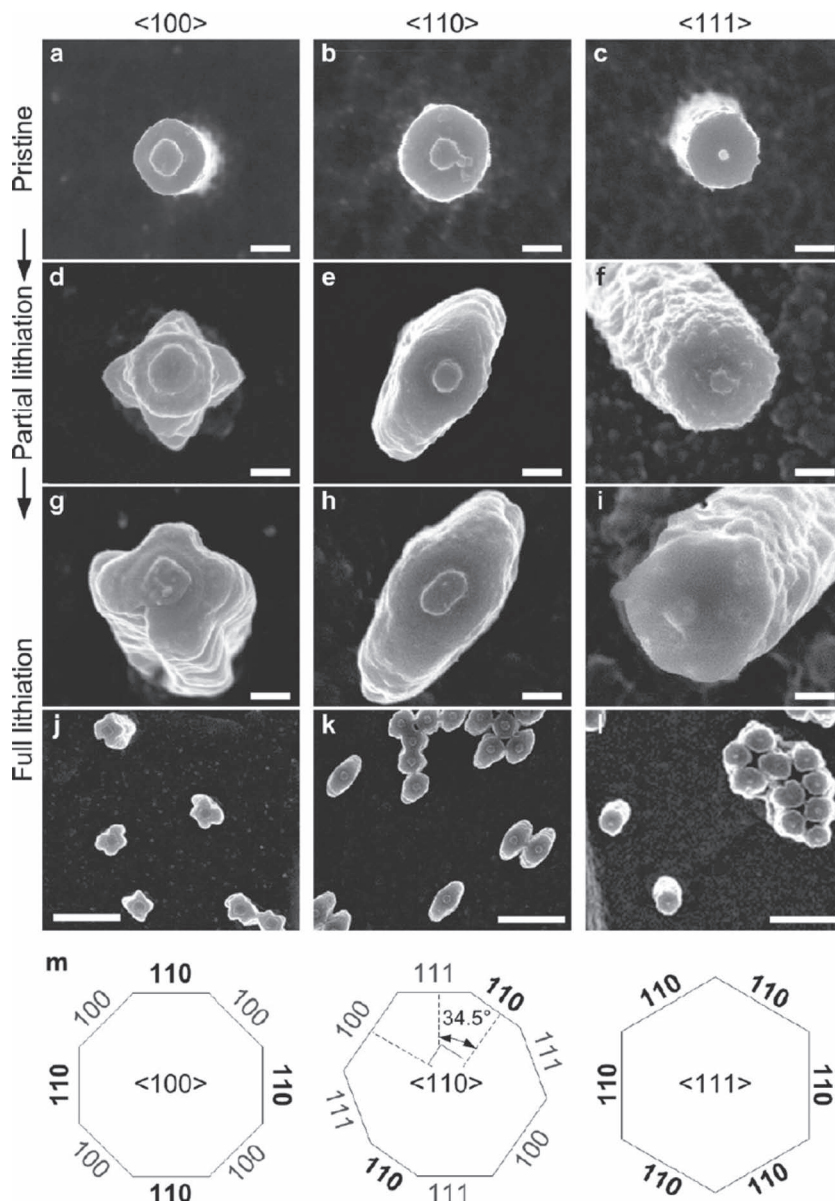


**Figure 2.** Fundamental mechanisms of Si lithiation reaction. Left panel: Anisotropic lateral expansion of crystalline Si nanopillars with different axial. The  $\langle 100 \rangle$  axially oriented pillars are shown in the left column,  $\langle 110 \rangle$  pillars are shown in the middle column, and  $\langle 111 \rangle$  pillars are shown in the right column. Reproduced with permission.<sup>[117]</sup> Copyright 2011, American Chemical Society.

electrolyte interfaces (SEI) and the degradation of the electrolyte. Single Si nanowires and nanorods provide a good opportunity to study the fundamental lithiation process. Recently, Lee et al. studied Si nanopillars with  $\langle 100 \rangle$ ,  $\langle 110 \rangle$  and  $\langle 111 \rangle$  axial orientations (Figure 2).<sup>[117]</sup> It is very interesting that the lithiation and volume expansion are quite anisotropic. There is a preferred large expansion along  $\langle 110 \rangle$  orientations, likely caused by the high speed Li ion diffusion along the  $\langle 100 \rangle$  orientation. As a result, the nanopillars expand along the lateral directions, but there is a shrinkage in height for the  $\langle 111 \rangle$  and  $\langle 100 \rangle$  oriented nanopillars. For  $\langle 110 \rangle$  oriented nanopillars, the height actually increases.

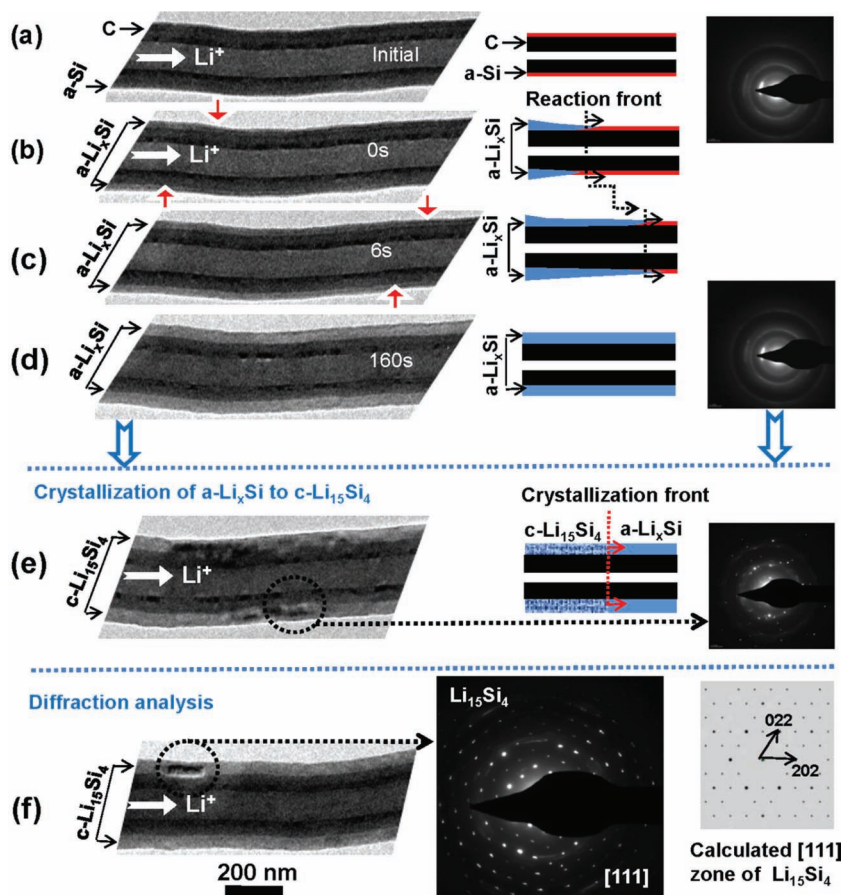


**Figure 3.** Microstructural evolution of the Si-carbon nanotubes during the charging.<sup>[122]</sup> The left column shows the TEM images, the middle column is a schematic drawing to guide the eye in reading the corresponding TEM images, and the right column is the selected area electron diffraction pattern. a) TEM image before the charge. b–f) The time-lapse TEM images showing the structural evolution. Reproduced with permission.<sup>[122]</sup> Copyright 2012, American Chemical Society.

Advanced characterization tools can also provide new lessons of the structural transition. Upon lithiation both crystalline and amorphous silicon will be transformed to an amorphous  $\text{Li}_x\text{Si}$  phase and subsequently a crystalline (Li, Si) compound, either  $\text{Li}_{15}\text{Si}_4$  or  $\text{Li}_{22}\text{Si}_5$ .<sup>[118–121]</sup> However, the detailed atomistic mechanism of such phase transitions has not been fully understood. If the phase transformation happens according to the classic nucleation and growth model, it will lead to composition fluctuation and phase separation in the amorphous that could have serious implications for the stability of the material during charge/discharge.<sup>[120,121]</sup> In situ TEM was used to study hollow carbon fibers coated with amorphous Si on both the exterior and interior surfaces as an anode.<sup>[122]</sup> It was found that the amorphous  $\text{Li}_x\text{Si}$  crystallizes to  $\text{Li}_{15}\text{Si}_4$  through a spontaneous, congruent process without long distance displacement and diffusion of the atoms (Figure 3). This mechanism is drastically different from what is expected from the classic nucleation and growth process which necessarily involves atomic diffusion, composition fluctuation and phase separation. The homogeneous phase transition may be another reason that the nanostructured material has better stability.

### 2.2.2. Membranes

Great emphasis has been placed on electrode materials, but much less attention has been paid to the fundamental understanding and rational design of membrane and separating materials. Such materials are critical for Li-ion batteries,<sup>[123,124]</sup> redox flow batteries,<sup>[125–128]</sup> Na-S batteries,<sup>[129]</sup> Li-S,<sup>[130]</sup> and Li-air batteries.<sup>[13,131]</sup> The functions of the membranes or separators are separating the complex ionic and molecular species, and allowing only the desired ions such as Li or Na ions, or the desired molecule, such as the oxygen molecules, to pass through without much difficulty. There is a great need to improve the conductivity, selectivity, and mechanical and chemical stability to improve the efficiency and reduce the cost.

The challenge in developing good ion conducting materials for the desired operating conditions can also be illustrated by the separation membranes in flow batteries to separate the electrolyte solutions.<sup>[125]</sup> In vanadium redox flow batteries (VRB) and most other flow batteries, a perfluorosulfonic acid (PFSA) polymer membrane, Nafion, is used.<sup>[132,133]</sup> The chemical structure of Nafion consists of a perfluorinated backbone with pendant vinyl ether side chains terminated with  $-\text{SO}_3\text{H}$  groups. This polymer contains both hydrophobic and hydrophilic regions and forms a two-phasic structure in a wet environment: a perfluorinated matrix that provides the chemical and mechanical stability to the membrane and a hydrophilic phase with a high density of sulfonic acid groups.

Recent studies (Figure 4a) revealed that hydrated Nafion membranes contain long, parallel, randomly packed water channels formed from inverted-micelle cylinders surrounded by partially hydrophilic side branches.<sup>[134]</sup> At a water content of  $\approx 20$  vol%, the water channels have diameters between 1.8 and 3.5 nm, with an average diameter of 2.4 nm. Such results are based on the information and parameters from small angle X-ray scattering (SAXS) measurements over a range of hydration, as well as from the water and proton self-diffusion coefficients obtained from pulsed-field gradient NMR experiments.<sup>[135]</sup> The wide parallel water channels confirm that the excellent proton conductivity is associated with water diffusion in Nafion.

However, these membrane materials are designed for polymer membrane fuel cell chemistry, for which the most significant challenges are water management, carbon monoxide poisoning of the electrocatalysts<sup>[136]</sup> and dismal high-temperature performance,<sup>[137,138]</sup> rather than for battery applications. For example, for VRBs, the main requirements are stability, good conductivity, and low cross-diffusion of ionic species other than protons. Nafion membranes have good conductivity for protons because of the wide water channels that allow water



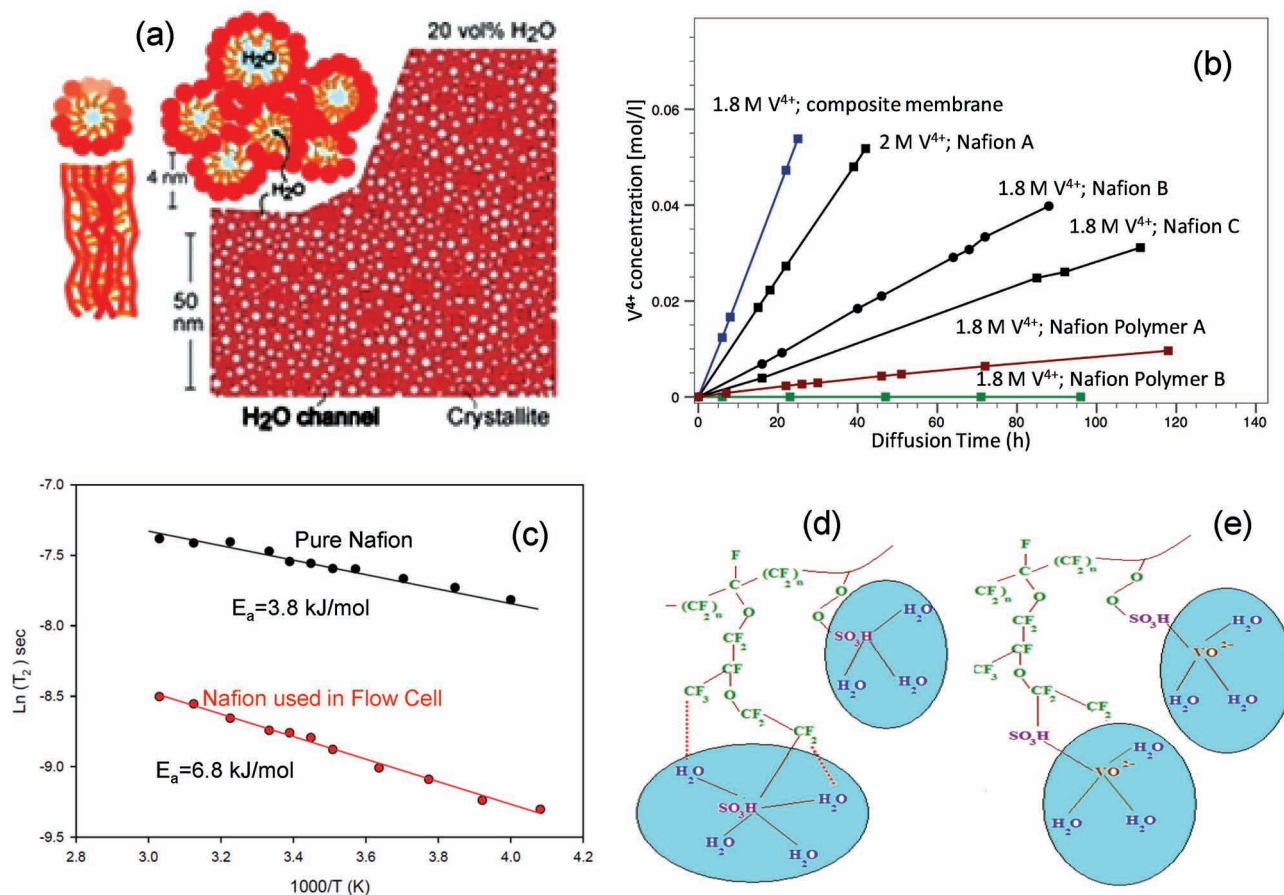


**Figure 4.** a) Randomly packed, 24 nm wide, parallel water channels in Nafion membranes for fast water diffusion and proton transport. Reproduced with permission.<sup>[134]</sup> Copyright 2008, Nature Publishing Group. b) Cross-diffusion of V<sup>4+</sup> in commercial and polymer modified membranes. Reproduced with permission.<sup>[142]</sup> Copyright 2011, Elsevier. Nafion Polymer A and Nafion Polymer B refer to polymerization of polypyrrole and polyaniline onto commercial Nafion membranes. c) NMR relaxation time of the V resonance peak as a function of temperature measured from NMR spectra showing the activation energy increased after soaking cell etching. d) Schematic of free Nafion polymers. e) Binding of V ions to the sulfate groups of Nafion as inferred from NMR measurements. Reproduced with permission.<sup>[143]</sup> Copyright 2011, Elsevier.

diffusion, but other hydrated cations can also diffuse through the membrane with the same mechanism, which gradually reduces the overall efficiency and capacity. Figure 4b shows the diffusion of V<sup>4+</sup> ions across different commercial Nafion membranes. Even a different pretreatment procedure can have a large effect on the V<sup>4+</sup> ion diffusivity. All the commercial membranes exhibit high diffusivity for V<sup>4+</sup> ions. Surface treatments (functionalization<sup>[139]</sup> or doping with inorganic particles<sup>[140]</sup>) and composite membranes (hybrid or multilayer)<sup>[141]</sup> have been investigated to either reduce the pore channel sizes or to introduce positively charged groups to repel the cations in order to decrease the V<sup>4+</sup> ion diffusion (Figure 4b),<sup>[142]</sup> but the long term effectiveness and durability of the new films are largely untested. Here, the results were obtained using a diffusion cell setup (78 mL 1.8 M V<sup>4+</sup>/4.5 M SO<sub>4</sub><sup>2-</sup> vs. 1.8 M Mg<sup>2+</sup>/4.5 M SO<sub>4</sub><sup>2-</sup>; diffusion concentration of V<sup>4+</sup> ions into the Mg<sup>2+</sup>-containing half cell were determined using UV-vis spectroscopy). Data for Nafion A, Nafion B, and Nafion C indicate diffusion of V<sup>4+</sup> ions through commercial Nafion membranes after different treatment, such as boiling in H<sub>2</sub>O or soaking in H<sub>2</sub>O at RT for different times before the diffusion test. Membrane modification

for data labeled “Nafion Polymer A” and “Nafion Polymer B” refers to polymerization of polypyrrole (pyrrole with hydrogen peroxide) and polyaniline (aniline chloride with ammonium persulfate), respectively, onto commercial Nafion membranes.

In addition, the proton conductivity in the redox flow cells significantly decreases over time, which has not been observed in fuel cell applications (Figure 4c).<sup>[143]</sup> We attributed this factor to the strong absorption of cations inside the membrane materials (Figure 4d,e). These cations are not present in a fuel cell environment. The degradation of the membrane over time is attributed to the binding of the cationic species to the sulfonic acid groups, as confirmed by NMR experiments.

Much effort has been put into developing alternative proton conductive membranes for fuel cell applications, such as alternative hydrocarbons, aromatic polymers, acid-doped base polymers, block copolymers, and chemically or physically modify the fluorinated polymers to form polymer-inorganic nanocomposites. The proton transport depends on the molecular chemistry (e.g., the backbone composition, the presence and length of side chains, the choice of the protogenic group) and the morphology of the hydrated membrane (e.g., degree of phase

separation, crystallinity). The diffusion of hydrated cations becomes more complex because of the heterogeneous nature of the polymer (i.e., co-organized crystalline and ionic domains), nano-confinement of the water subject to a high density of tethered anionic groups (e.g.,  $-\text{SO}_3^-$ ), and hydration and complex speciations of the cations. Much less effort has been made to rationally design and synthesize ion-conductive membranes for battery applications with minimum cross-contamination, good chemical and mechanical stability, and low cost based on the understanding of the relationships between the molecular and microstructure, morphology, ionic conductivity, and transport of hydrated ions.

### 2.3. Electrolyte Chemistry

All electrochemical devices involve tailored electrolytes. In particular, many energy storage devices usually involve aggressive electrochemical environments, molten salts, concentrated electrolyte solutions, and complex electrochemical reactions that are poorly understood. A common problem is the difficult to control the chemical separation, solubility, precipitation, and reactions in the electrolytes. In VRBs, the poor solubility of the V species limits the energy density. In Li-S batteries, the dissolution of the polysulfides causes fast fading of the capacity.<sup>[8,9,144,145]</sup> In Li-air batteries, the stability of the electrolytes is a big problem.

In VRBs, vanadium cation concentrations are generally limited to 2 M, which is determined by the precipitation of  $\text{V}^{3+}$  ions in the anolyte at below 10 °C and the formation of insoluble  $\text{V}_2\text{O}_5$  from  $\text{V}^{5+}$  ions above 40 °C in the catholyte.<sup>[146]</sup> As a result, the energy density of VRBs is only about 25 Wh/kg, as compared with 150 Wh/kg in state-of-the-art Li-ion batteries. There have been numerous efforts to increase the energy density by modifying the electrolyte or changing the electrolyte chemistry, such as using a halide solution and vanadium/bromide redox couples,<sup>[147]</sup> but any change or modification in the electrolyte chemistry also changes the redox chemistry and most alterations produce undesirable side reactions. Many inorganic and organic additives have been used to improve the solubility and activity of the concentrated electrolyte solutions.<sup>[148]</sup> There has been limited understanding of the exact role of these additives on the chemical speciation and redox reactions of the cations. In many cases, the reports on the effects of the additives are contradictory from one study to another.

Recently, a mixed electrolyte VRB system was reported using electrolyte solutions containing both sulfate and chloride anions.<sup>[149]</sup> This VRB system shows a 70% increase in energy capacity compared to the conventional all-vanadium RFB, which employs only sulfuric acid to solubilize the  $\text{V}^{x+}$  species. In this novel electrolyte  $\text{V}^{4+}$  ions and  $\text{V}^{5+}$  ions are stabilized by 6 M  $\text{Cl}^-$  anions while 2.5 M  $\text{SO}_4^{2-}$  anions help stabilize  $\text{V}^{3+}$  ions over a wider temperature range.  $\text{V}^{2+}$  ions do not exhibit any stability issues in either the mixed electrolyte or pure HCl or  $\text{H}_2\text{SO}_4$ . The system has been demonstrated to operate from –5 to +50 °C, with an energy efficiency of 87% (over 20 days).

To improve the properties of the electrolyte and control the long-term stability, a much better understanding of the concentrated solution chemistry is required. In addition, chemical species and their interactions, affecting the solubility and redox

reactions, need to be better investigated. The vanadium species in an aqueous solution is sensitive to the pH,  $\text{V}^{x+}$  ion concentration, temperature, and many other factors. Figure 5a,b shows the possible redox reaction on the positive and negative sides and the equilibrium species of  $\text{V}^{x+}$  ions as a function of pH and  $\text{V}^{x+}$  ion concentration.<sup>[150]</sup> Here the electrochemical activity as a function of V concentration was measured by the redox current by cyclic voltammetry scan (0.2 to 1.6 V at 50 mV/s) at 1.1 V in  $\text{V}^{4+}$  solution (5 M  $\text{H}_2\text{SO}_4$ ).  $^1\text{H}$  NMR spectra of vanadium (IV) electrolyte solutions were measured at 300 K using 11.7 T magnetic field for different vanadium (IV) concentrations, illustrating that  $^1\text{H}$  NMR (both the peak position and the peak line width) is sensitive to the changes of vanadium ion concentration. The coordination chemistry of V ions with water and the redox reaction involving water exchange was based on variable temperature  $^1\text{H}$  and  $^{17}\text{O}$  NMR on electrolyte solution with different vanadium ion concentrations and theoretical calculation using density functional theory.<sup>[151]</sup>

As seen from the figure,  $\text{V}^{x+}$  ions should not exist as single cations in concentrated solution, which determines the electrochemical activity, but a systematic understanding of the chemical species and the redox reaction processes at high acid and high  $\text{V}^{x+}$  ion concentrations are still lacking. At high  $\text{V}^{x+}$  ion and acid concentrations, sulfate or halide complexes, dimers, or chain-like vanadate clusters have been proposed.<sup>[152–155]</sup>

The electrochemical activity does not increase linearly with the  $\text{V}^{x+}$  ion concentrations (Figure 5c). A plateau in activity is observed even before the solubility limit is reached. Interpreting the fine structures of advanced nuclear magnetic resonance measurements could provide a possible explanation for this observed plateau in activity. Variable temperature  $^1\text{H}$  and  $^{17}\text{O}$  NMR studies on electrolytes with different concentrations of the active vanadium species reveal that the soluble  $\text{V}^{4+}$  ions ( $\text{V}^{5+}$  ions show similar results) exist in the forms of hydrated vanadyl ions, i.e.,  $[\text{VO}(\text{H}_2\text{O})_5]^{2+}$  (Figure 5d and inset in Figure 5a),<sup>[151]</sup> with the  $\text{V}^{4+}$  ion in an octahedral coordination with the vanadyl oxygen in the axial position, the remaining five coordination positions are occupied by water molecules. This hydrated vanadyl ion structure is stable for up to 3 M concentrated solutions and in the temperature range of 240 to 340 K. The sulfate anions in the electrolyte solutions are found to be weakly bound to this hydrated vanadyl ion and occupy its second coordination sphere. The exchange of the  $\text{H}_2\text{O}$  molecules between the V-bonded  $\text{H}_2\text{O}$  and the free bulk water has been confirmed by NMR, where the exchange of the axial  $\text{H}_2\text{O}$  is found to be faster than that of the planar  $\text{H}_2\text{O}$  molecules. This is due to the slightly longer bond distance between the  $\text{V}^{4+}$  ion and the axial  $\text{H}_2\text{O}$  compared with the bond length between the  $\text{V}^{4+}$  ion and  $\text{H}_2\text{O}$  molecules in cis-positions to the vanadyl oxygen. The charge/discharge ( $\text{V}^{x+}$  ion oxidation/reduction) is accompanied by losing (oxidation) or obtaining (reduction) one  $\text{H}_2\text{O}$  molecule from the vanadyl ion coordination sphere. The exchange of both the V-bonded axial and the planar water molecule in the hydrated vanadyl ion with free bulk water molecules, including the likelihood of intra molecular  $\text{H}_2\text{O}$  exchange within the hydrated vanadyl ion, plays a critical role in the performance of VRBs. At a higher  $\text{V}^{x+}$  ion concentrations, more water molecules are bound to the  $\text{V}^{x+}$  ions, leaving behind less bulk water for a water exchange reaction. In addition, the number of



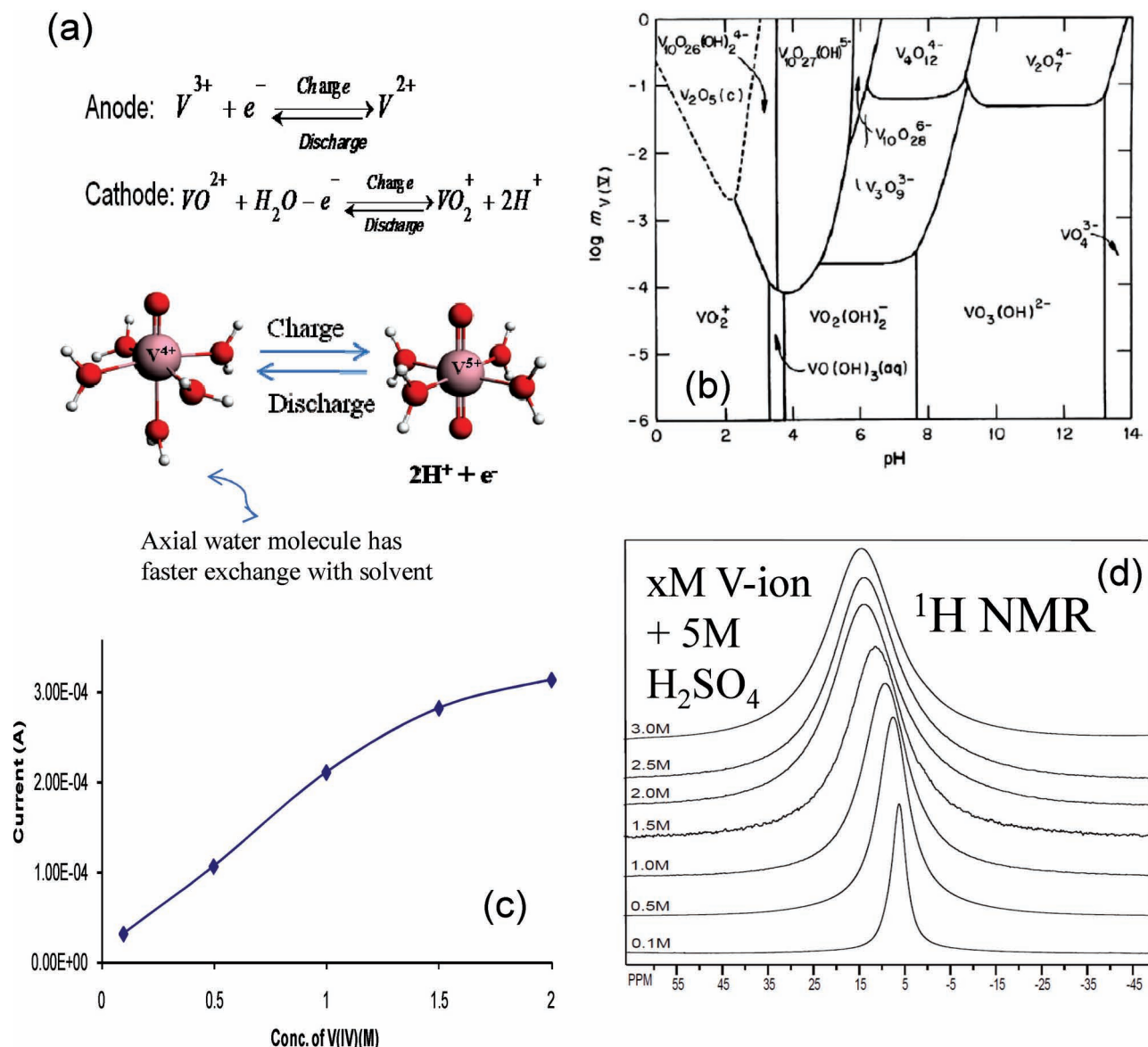


**Figure 5.** VRB batteries and the chemical speciation involved. a) The redox reaction on the cathode and anode sides of VRB. b) V chemical species as a function of pH and V concentration. Reproduced with permission.<sup>[150]</sup> Copyright 1998, Robert Krieger Publishing Company. c) Electrochemical activity as a function of V concentration. The inset in (c) shows the coordination chemistry of V ions with water and the redox reaction involving water exchanged. d)  $^1\text{H}$  NMR spectra of vanadium (IV) electrolyte solutions. Reproduced with permission.<sup>[151]</sup> Copyright 2010, Elsevier.

sulfate anions that are weakly bound to hydrated vanadyl ions increases, which further hinders the  $\text{H}_2\text{O}$  exchange process. As a result, a plateau in electrochemical activity is observed before the solubility is reached.

#### 2.4. New Battery Design

New electrode materials and electrode designs may bring breakthroughs in old technologies. For example, lead acid batteries have been around since the 1800s, are currently widely used, and are among the least expensive by capital. However, lead acid batteries have low energy and power density and they can only be used for a shallow charge-discharge cycle. They also

have a short life span because of lead sulfate precipitation, dissolution and reprecipitation of lead, and other severe corrosion problems. This, in addition to extra maintenance requirements, makes this technology an overall expensive option for large-scale energy storage in the long run.

A recent development in lead acid battery research, however, has the potential for long life applications. This new technology is called the lead carbon battery, ultrabattery, or hybrid battery.<sup>[156–159]</sup> In a conventional lead acid battery, a positive electrode made of lead dioxide and a negative electrode of metallic lead are immersed in dilute sulfuric acid electrolyte solutions.<sup>[156–159]</sup> In the lead carbon battery, the negative electrode is partially replaced or combined with high-surface-area activated carbon. As shown in Figure 6a, the carbon modification

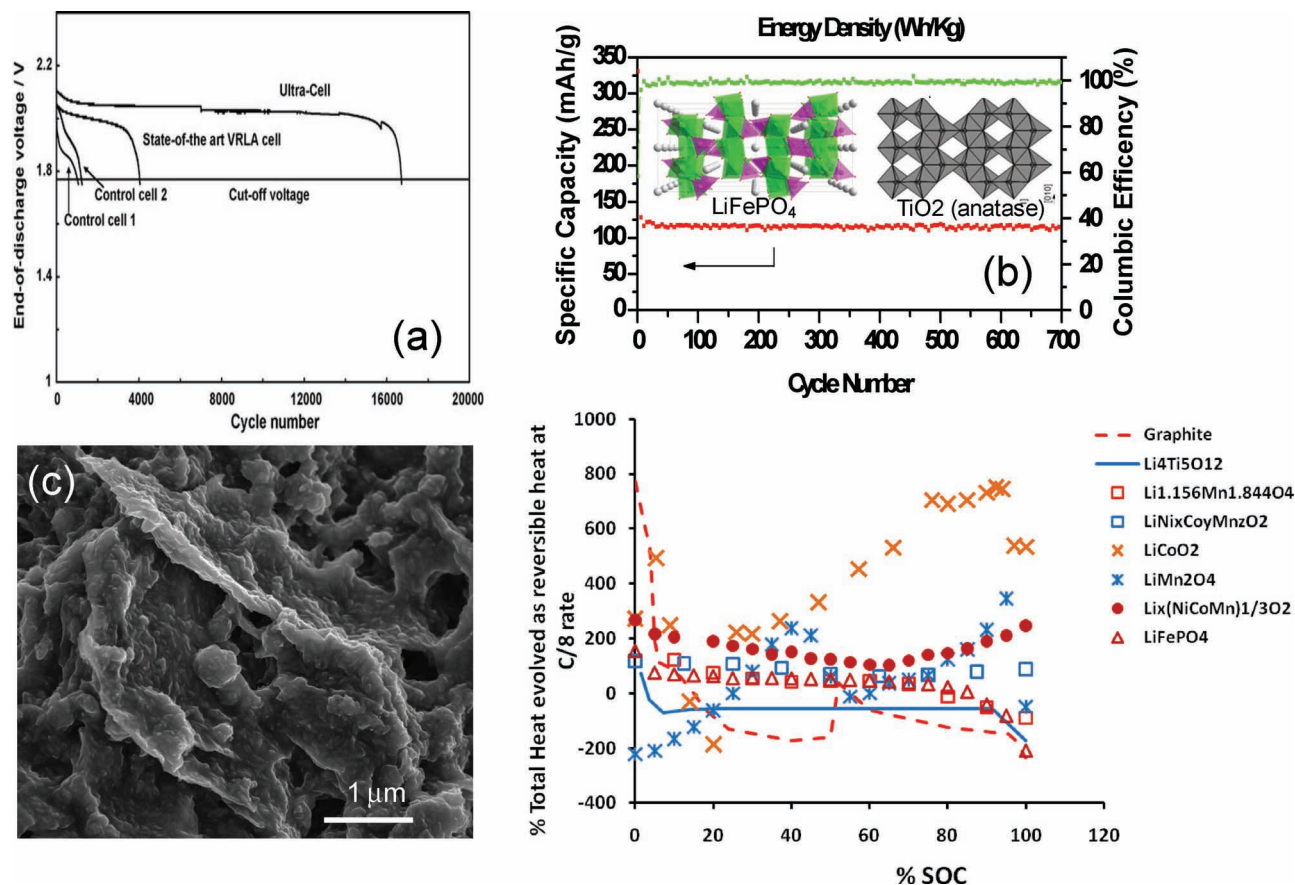


**Figure 6.** New chemistry from traditional batteries. a) Comparison of traditional lead acid battery and new lead carbon battery. Reproduced with permission.<sup>[156]</sup> Copyright 2006, Elsevier. b) Stability of LiFePO<sub>4</sub>-TiO<sub>2</sub> Li-ion battery combination. Reproduced with permission.<sup>[168]</sup> Copyright 2010, Elsevier. c) TiO<sub>2</sub>-graphene nanocomposites. Reproduced with permission.<sup>[169]</sup> Copyright 2009, American Chemical Society. d) Heat generation of various cathode and anode materials in Li-ion batteries. Reproduced with permission.<sup>[171]</sup> Copyright 2009, Elsevier.

significantly extended the life of the battery. The exact role of the carbon is still under debate, but it has been suggested that the high-surface-area carbon electrode functions as an electrical double layer supercapacitor and is capable of quickly storing and releasing a large amount of energy. This not only increases the power density, but also prevents the degradation of the electrode materials because of lead sulfate precipitation (also called “sulfation”) that occurs during deep charge/discharge cycles.<sup>[156–159]</sup>

Li-ion batteries have been developed for small power electronics and are now favorably considered for automotive applications because of the high energy density.<sup>[4,160]</sup> In contrast to vehicle applications, stationary applications place a higher value on reducing the technology cost and achieving the decades-long durability that utilities typically expect of their assets. Several issues need to be addressed for stationary storage. First, safety in Li-ion batteries is still a concern. The lithiated-graphite electrode operates at a potential close to that of metallic lithium, leading to Li-dendrite growth and thereby potential electrical short circuit. Second, the calendar and cycle life are still too short and durability remains an issue. Most important of all, the cost is still around \$1000/kWh, which is too high for most commercial applications.

One approach to solve the problem of Li-ion batteries for the stationary market is to use different electrode materials that are less expensive, but more durable performance.<sup>[161–166]</sup> One important candidate is a TiO<sub>2</sub>-based anode.<sup>[161]</sup> TiO<sub>2</sub> is an abundant and low-cost material and is already widely used in a number of applications, including pigments, paints, sunscreens, catalysis, and more advanced applications. Typically, a TiO<sub>2</sub> or lithium titanate anode operates at 1.55 V and can accommodate Li with a theoretical capacity of 175 mAh/g or higher. The high voltage will reduce the energy density, but is intrinsically safer compared to graphite. During charge/discharge, TiO<sub>2</sub> is transformed into lithium titanate with a 3D network of channels for facile Li<sup>+</sup> diffusion and exhibits little or no volume expansion/extraction. Exceptional stability over thousands of cycles has been demonstrated for TiO<sub>2</sub> and titanate materials. We also showed that commercial TiO<sub>2</sub>, such as P25, can be directly used as the anode material without any thermal or chemical treatment and has excellent electrochemical activity and stability.

The TiO<sub>2</sub> can be used in conjunction with LiFePO<sub>4</sub> cathode material. This assembled full cell can operate at ≈3.5 V vs. Li, with a high capacity of about 170 mAh/g.<sup>[167]</sup> Figure 6b shows the performance of the combination of the LiFePO<sub>4</sub> cathode and TiO<sub>2</sub> anode material with excellent stability.<sup>[168]</sup> A small

amount of graphene (molecularly exfoliated graphite sheets) is added to the  $\text{TiO}_2$  to improve the conductivity of the materials (Figure 6c).<sup>[169]</sup> Recently, other inexpensive cathode materials, such as  $\text{LiMn}_2\text{O}_4$  (spinel), are also being investigated for similar applications.<sup>[170]</sup>

Another factor is the heat management, which becomes especially important with large battery sizes,<sup>[171]</sup> and batteries for stationary or distributed energy storage at the consumer end are expected to operate without active cooling. Thermal management becomes more critical because the surface area/volume ratio of these batteries decreases with increasing battery size, resulting in a lower heat transfer rate per unit rate of heat generation. The entropy change,  $\Delta S$ , can contribute up to 1.5 to 2 times the irreversible heat-generation rate at the 1 C rate, and as much as 5 to 8 times the irreversible heat-generation rate at C/8 rates.<sup>[171]</sup>

As shown in Figure 6d, the reversible heat-generations at C/8 rate for various anode and cathode combinations can be quantified across the state of charge (SOC) or depth of charge range.<sup>[172]</sup> For anodes, the energy loss of lithium titanates due to irreversible heat is lower compared to that of graphite. For cathodes,  $\text{LiCoO}_2$  has the highest reversible heat-generation rate component. At a certain SOC range, the reversible heat component can be very high. This information can serve as a tool for the battery management system to control battery load or charge current at various SOC, such that high-temperature excursions are effectively prevented. While the internal resistance can be minimized by suitable electrode and cell design, the reversible heat-generation rate can play a significant role, especially in cases where internal resistance has been minimized. Hence, the measurement of individual electrode and full cell entropy change is expected to contribute significantly to effective thermal management for large batteries.

Na-S and Na-metal hybrid batteries depend on  $\text{Na}^+$  ion conductors. The synthesis of  $\text{Na}^+$  ion conductive materials that can operate at temperatures below 300 °C, or even approaching room temperature, is a major challenge for such technologies. The crystalline structure of  $\beta''$ -alumina is based on stacked spinel block structures, with the  $\text{Na}^+$  ion transport mainly going through the ab planes between the spinel blocks. The properties of  $\beta''$ -alumina depend on the levels of impurities, such as MgO, the grain sizes, the density, the orientation of the grains, and the thickness of the membrane,<sup>[173]</sup> but so far good conductivity is only achievable at above 300 °C. In the Ceramtec design, Nasicon (Na super ionic conductor) is used as the solid-state,  $\text{Na}^+$  ion conducting membrane. Nasicon represents a class of materials with the general formula  $\text{AM}_2(\text{PO}_4)_3$ , where A is the monovalent cation and M the tetravalent cation.<sup>[174]</sup> The phosphate anions can be partially replaced by silicate. This class of materials has reasonable  $\text{Na}^+$  ion conductivity over a temperature range from 150 °C to 300 °C, but the conductivity ( $10^{-6}$  S/cm to  $10^{-4}$  S/cm) is orders of magnitude lower than what can be obtained from typical polymer proton conducting materials, such as Nafion ( $10^{-2}$  S/cm to  $10^{-4}$  S/cm). New approaches to a rational design of the crystalline structure and the ion conducting channels and to control the charge distribution in the framework are desired for next generation ion conducting materials.

There are several approaches to reduce the operating temperatures and cost. One new design is planar rather than

tubular (Figure 7a).<sup>[175,176]</sup> The planar design can solve two problems. First, the solid electrolyte membrane can be made from traditional ceramic processing techniques, such as tape casting. This would greatly reduce the complexity of the manufacturing process and the associated cost. Second, it is possible to make much thinner membranes (Figure 7b). The thinner membranes provide better conductivity at a lower temperature and thus allow the device to operate at a more moderate temperature range (200 to 250 °C). The concept of the planar Na MH battery has been recently demonstrated (Figure 7c). The prototype device shows good conductivity and good charge-discharge reversibility, and energy density of 100 Whr/kg has been demonstrated.

### 3. Emerging Energy Storage Technologies and Perspectives

As discussed, although some technologies show good promise for transportation and stationary applications, achieving the ultimate energy density, near 100% efficiency and the ultralow cost is still a great challenge. New Li-S and Li-air batteries have very high theoretical energy density, but their reversibility, efficiency and cost are still problematic. Large-scale energy storage with sodium ion or other common, inexpensive chemicals at low temperatures is attractive not only because of the abundance and low cost of these materials, but also because of the environmental concerns for technologies using devices operated under aggressive electrochemical conditions.

#### 3.1. Lithium-Sulfur and Lithium-Air Batteries

##### 3.1.1. Li-S Chemistry

Among emerging battery systems, lithium-sulfur (Li-S) batteries have attracted considerable attention.<sup>[177,178]</sup> Elemental sulfur is abundant and has high theoretical capacity ( $1675 \text{ mAh g}^{-1}$ ) and specific energy ( $2600 \text{ Wh kg}^{-1}$ ). In addition, sulfur is also low cost and environmentally friendly. Despite these advantages, practical applications of Li-S batteries are limited by several problems. One is the electrical insulating nature of elemental sulfur ( $5 \times 10^{-30} \text{ S cm}^{-1}$  at 25 °C) and the reaction products of the discharge process, which lower both the electrochemical activity and the utilization of sulfur.<sup>[144,179]</sup> Another is poor cyclability, which results from the high solubility of the intermediate product, lithium polysulfide  $\text{Li}_2\text{S}_x$  ( $2 \leq x \leq 8$ ), formed during both the discharging and charging processes.<sup>[144,145,180]</sup> Dissolved polysulfides can diffuse to the lithium anode where they are reduced to short-chain polysulfides. Those soluble species also can move back to the cathode and be reoxidized into long-chain polysulfides. This parasitic process creates an internal shuttle reaction that results in low coulombic efficiency. Moreover, a fraction of the soluble polysulfides are strongly reduced to insoluble  $\text{Li}_2\text{S}_2$  and/or  $\text{Li}_2\text{S}$ , which are then deposited on the anode surface and gradually form a thick layer during repeated cycling. The same phenomenon also occurs on the cathode surface during discharging. The deactivated insoluble agglomerates on both electrodes can lead to a progressive loss of active



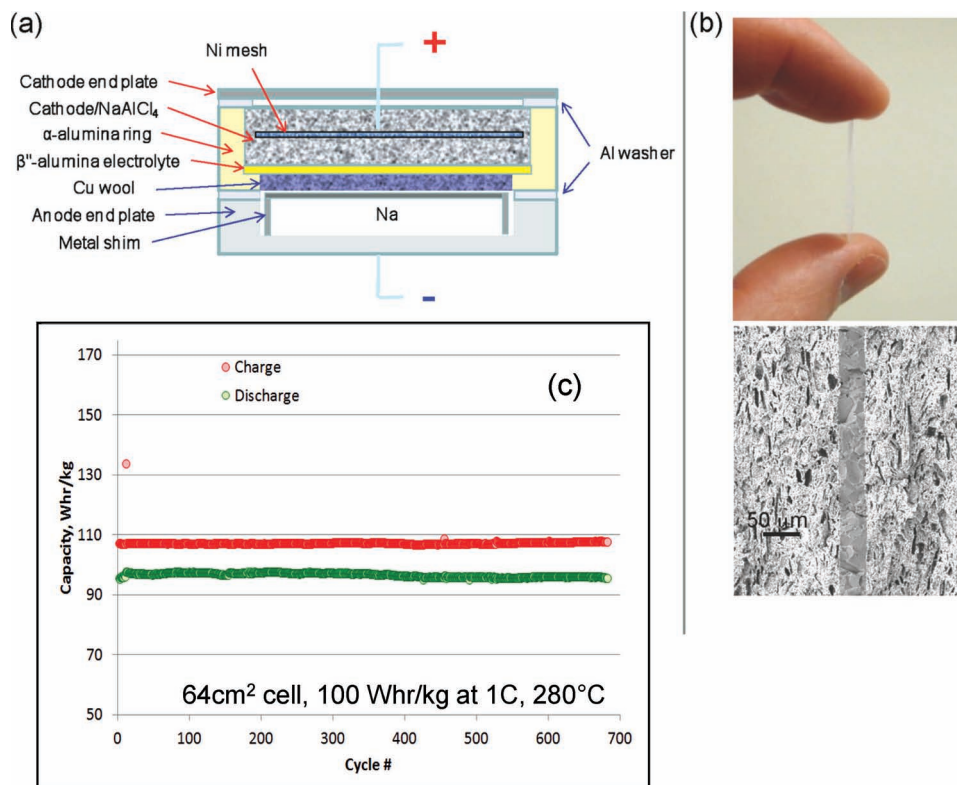


**Figure 7.** Planar Na-MH battery: a) design schematic; b) thin  $\beta''$ - $\text{Al}_2\text{O}_3$  membrane from tape casting and co-sintering with  $\text{ZrO}_2$  (top panel) and SEM image of the  $\beta''$ - $\text{Al}_2\text{O}_3$  membrane sandwiched between a  $\text{ZrO}_2$  porous support (bottom panel); and c) cycling results on the charge–discharge cycles of a planar Na-MH battery. Reproduced with permission.<sup>[252]</sup> Copyright 2010, The Electrochemical Society.

materials, inaccessibility of the active components in the interior sulfur electrode, degradation of the electrode structure, and increased cell impedance. These cumulative effects then are reflected in the rapid capacity degradation of the Li-S battery upon discharge/charging cycling.

One approach to solve these above-mentioned problems is to use alternative electrolytes and electrolyte additives to mitigate the solubility problem of the polysulfides in the electrolyte.<sup>[181–183]</sup> The other approach is to tailor the conductive matrix to support good conductivity and dispersion of sulfur and also constrain sulfur and the polysulfides within the framework.<sup>[8,9]</sup> The latter approach has been extensively considered because it may solve both the conductivity and solubility problems. Many different porous carbon materials have been studied.<sup>[145,178,184–188]</sup> Nazar et al.<sup>[178]</sup> used ordered mesoporous carbon to encapsulate the sulfur species within resident nano-channels. This composite, which was coated with an additional thin-layer polymer, showed a high initial reversible capacity of  $1320 \text{ mAh g}^{-1}$  with promise cycling ability. Most recently, porous hollow carbon spheres with an interior void space and a mesoporous shell structure composed of sulfur exhibited a high initial reversible capacity of  $1071 \text{ mAh g}^{-1}$  at a  $0.5 \text{ C}$  rate and maintained 91% capacity retention after 100 cycles.<sup>[189]</sup> Several groups have reported extended cycling of porous carbon/sulfur composites. Sun et al.<sup>[190]</sup> developed a bimodal mesoporous carbon/sulfur electrode that manifested 400 full cycles without dramatic electrode failure. Gao et al.<sup>[184]</sup> synthesized carbon

spheres with abundant narrow micropores. Sulfur loaded into the micropores barely escaped. The as-fractured composite delivered a sustainable reversible capacity of  $650 \text{ mAh g}^{-1}$  at  $400 \text{ mA g}^{-1}$  for hundreds of cycles. Furthermore, several groups have also reported the use of graphene sheets to confine the sulfur compounds.<sup>[144,188,191]</sup>

Conductive polymers, such as polythiophene and polypyrrole with different tailored porosities, have been explored as matrices to physically absorb and hold sulfur.<sup>[192–196]</sup> Wu et al.<sup>[193]</sup> constructed a sulfur/polythiophene composite with a core/shell structure. The composite produced a high initial discharge capacity of  $1119 \text{ mA g}^{-1}$  and can retained 69.5% of the capacity retention after 80 discharging/charging cycles. Several groups have explored polyacrylonitrile (PAN)/S systems.<sup>[197–200]</sup> It was reported that the PAN became dehydrogenated and cyclized at  $450^\circ\text{C}$  and all the sulfur reacted with the PAN to form a heterocyclic polymer interconnected with disulfide bonds on the side chain. The chemically bonded sulfur shows good cycling retention of 90% up to 380 cycles,<sup>[200]</sup> but the capacity ( $470 \text{ mAh g}^{-1}$ ) and operating voltage (lower than  $2.0 \text{ V}$ ) are relatively low. Recently, Xiao et al. reported the synthesis of self-assembled polyaniline hollow nanowires (PANI-HNW) for sulfur encapsulation.<sup>[9]</sup> The polymer forms a 3D, cross-linked, structurally-stable sulfur-polyaniline (SPANI) polymer backbone with both inter- and/or intrachain disulfide bonds interconnected through in situ vulcanization. This SPANI-HNW polymer molecular framework provides strong physical and

chemical confinement to the elemental sulfur and the resident polysulfide. In addition, the soft polymer matrix and nanostructures developed in this study can allow reversible in situ deposition of intermediate polysulfide species during discharge and their subsequent transformation during recharging within the polymer matrix, and accommodate the volumetric change accompanying the electrochemical reactions. As a result, the as-synthesized SPANI-HNW/S composite exhibited superior discharge/charging cycling stability and rate capability. The electrode could retain a discharge capacity of 837 mAh g<sup>-1</sup> after 100 cycles at a 0.1 C rate. Even at a high discharge rate of 1 C, the electrode still manifest a very stable cycling performance for up to 500 cycles.<sup>[9]</sup>

### 3.1.2. Lithium-Air Batteries

Li-air battery is another promising rechargeable Li battery technology. It converts the chemical energy in lithium (anode) and oxygen (cathode) into electric energy during discharge (similar to a fuel cell, but the fuel is lithium instead of hydrogen) and it stores electric energy by splitting Li-O<sub>2</sub> discharge products (ideally, Li<sub>2</sub>O<sub>2</sub> in nonaqueous system and LiOH in aqueous system) during charge using electricity (similar to an electrolysis device or a reversible fuel cell to generate hydrogen and oxygen by splitting water).<sup>[201–207]</sup> Since lithium air batteries combines the challenges of (reversible) fuel cells and batteries,<sup>[10,13,208–213]</sup> the technology is far from practical application due to its low power density, poor cycling capability, and low energy efficiency.<sup>[11,12,209,210,214]</sup> Oxygen electrocatalyst is one of the most challenging tasks in developing lithium air battery. Other important challenges also exist in lithium metal anode (dendrite formation, incompatibility with electrolyte and air),<sup>[215]</sup> electrolytes (instability in oxygen-rich electrochemical conditions, conductivity, evaporation for nonaqueous electrolytes),<sup>[216–218]</sup> etc. These challenges are discussed in more details in a separate article.<sup>[251]</sup>

## 3.2. Ultralow Cost Batteries?

### 3.2.1. Na-Ion Batteries

Currently, most devices use expensive and toxic materials such as Li to store energy. Scientists have long been asking if it is possible to store energy using relatively inexpensive, naturally abundant, and environmentally benign materials, such as Na ions. The working principle of the Na ion battery system is in principle similar to that of Li-ion battery, which depends on the shuttle of Na ion in the structural channels of the anode and cathode. The progress and challenges in Na-ion batteries are discussed in detail in another article. In brief, Na ions are about 55% larger than Li ions. This makes it difficult to find a suitable host material to accommodate Na ions and allows reversible and rapid ion insertion and extraction.<sup>[219]</sup> Nanostructures can improve the properties of energy storage materials.<sup>[220–223]</sup> Recently, Kim et al.<sup>[221]</sup> reported a layer-structured Na<sub>0.85</sub>Li<sub>0.15</sub>Ni<sub>0.21</sub>Mn<sub>0.64</sub>O<sub>2</sub> material as cathode with a capacity of about 95 mAh g<sup>-1</sup> and good capacity retention over 50 cycles. More recently, Cao et al. reported a single crystalline Na<sub>4</sub>Mn<sub>9</sub>O<sub>18</sub>

nanowire material with an orthorhombic lattice structure, and with a reversible capacity of 128 mAh g<sup>-1</sup> and stable cycling for over 1000 cycles (Figure 8a).<sup>[220]</sup>

For anode materials, early efforts involving metallic Na suffered from dendrital growth problems. Graphite has poor intercalation property for large Na ions. Hard carbon has been reported to deliver capacities up to 300 mAh g<sup>-1</sup> because Na ions can absorb onto the surfaces of nanopores.<sup>[224–229]</sup> However, the reversibility of this material is still a challenge. Recently, Dahn et al.<sup>[230]</sup> showed that the Na-intercalated hard carbon (Na<sub>x</sub>C) has higher reactivity with the non-aqueous electrolyte than that of Li<sub>x</sub>C<sub>6</sub>, raising new concerns of the instability of the electrolyte. Theoretically, like Li alloys, which have been extensively investigated as high capacity anodes for Li-ion batteries,<sup>[66,231–235]</sup> Na can alloy with many metallic elements such as Sn, Sb, germanium (Ge), lead (Pb), and the calculated theoretical specific capacities are 847 (Na<sub>15</sub>Sn<sub>4</sub>), 660 (Na<sub>3</sub>Sb), 1108 (Na<sub>3</sub>Ge), and 484 (Na<sub>15</sub>Pb<sub>4</sub>) mAh g<sup>-1</sup> respectively.<sup>[236]</sup> Indeed, recently, Xiao et al. reported, for the first time, high capacity alloy reaction for Na ion insertion based on SnSb/C nanocomposites with a reversible capacity over 500 mAh g<sup>-1</sup> (Figure 8b).<sup>[237]</sup>

### 3.2.2. Batteries Based on MOFs

The search for ultralow cost, environmental friendly energy storage mechanisms will never stop. Prussian blue, normally MFe<sup>3+</sup>Fe<sup>2+</sup>(CN)<sub>6</sub>, was discovered in the 1700s and has been widely used for pigments and paints and even as sequestering agents for heavy metal poisons in medicine, with an annual production capacity of over 12 000 tons. This material is inexpensive and also environmentally friendly. In one study, copper hexacyanoferrate nanoparticles were prepared as the active electrode material. This material has an open-organic-framework (MOF) structure (Figure 8C), and can tolerate high strain during the redox reaction. This material can be cycled for over 40 000 charge/discharge cycles at 17C rate and retain 83% of the initial capacity. These types of materials may have great potential for low cost, large scale stationary application. However, the energy density is still rather low (about 50 mAh/g) as compared to other technologies (Figure 8d).<sup>[238]</sup>

## 3.3. Lessons from Biology

Biological systems have evolved to integrate all functions associated with the capture, storage, and use of a wide range of energy sources (optical, electrical, mechanical, and chemical). There are important lessons not only for materials design and synthesis, but also for building new energy storage devices.<sup>[239]</sup> For example, ion channels play an important role in cells and their properties are unmatched by synthetic membranes in terms of selectivity, efficiency and kinetics. Proton transport through transmembrane proton channels can be 15 times faster than that of other ions (K<sup>+</sup>) and 8 times faster than that of water molecules.<sup>[240]</sup> Faster proton transport was achieved through a concerted fast diffusion mechanism along single water molecular wires.<sup>[240–242]</sup> On the other hand, in biological water channels, only water molecules are allowed to go through, partially because of the positive charge in the channels. Selective

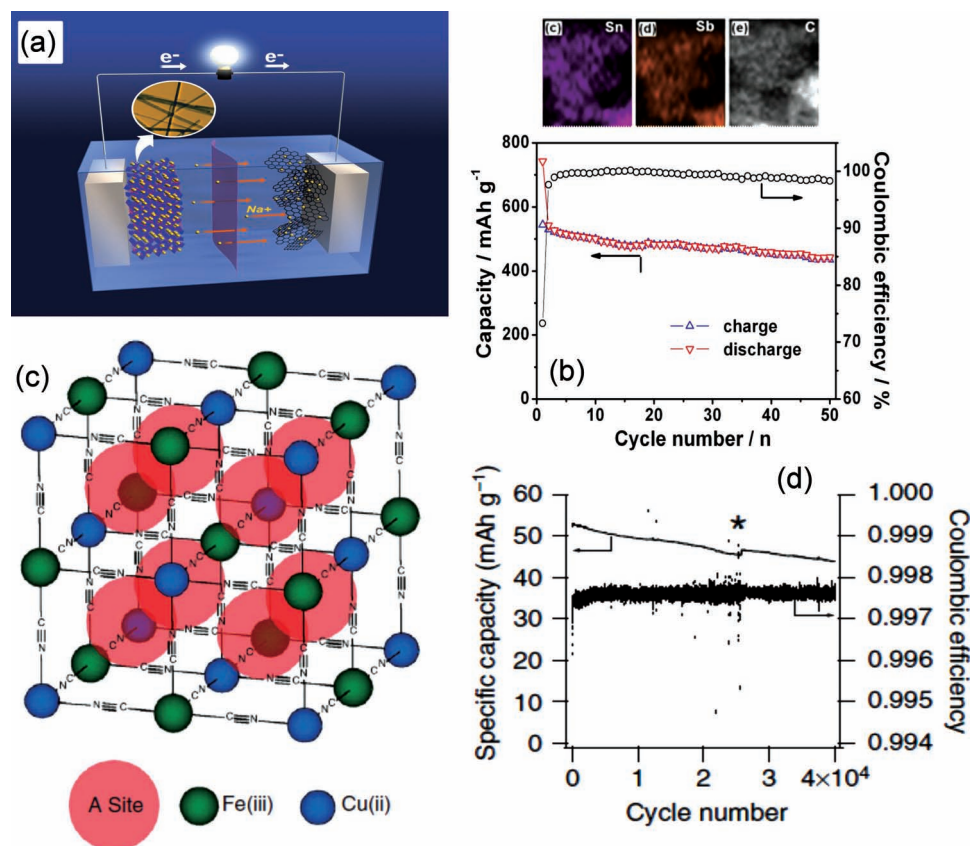


**Figure 8.** Na-ion batteries and CuHCF batteries. a) Schematic of a Na-ion battery made of single crystalline nanowire as the anode and hard carbon as the cathode. Reproduced with permission.<sup>[220]</sup> b) Cycling performance of the SnSb/C nanocomposite electrode at a cycling rate of 100 mA g<sup>-1</sup>. The colored images above show the nanoscale distribution of Sn, Sb, and C respectively. Reproduced with permission.<sup>[237]</sup> Copyright 2012, Royal Society of Chemistry. c) The 3D network of CuHCF. d) Long-term cycling of CuHCF at a 17 C-rate between 0.8 and 1.2 V shows 83% capacity retention after 40 000 cycles, with 99.7% coulombic efficiency. Reproduced with permission.<sup>[238]</sup> Copyright 2011, Nature Publishing Group.

cation diffusion in ion channels is accomplished by structurally matching the coordinates with the cations, hydrophobic-hydrophilic interactions, and channel sizes.<sup>[243]</sup> The biological ion channels give clues on how to design synthetic materials (membranes, separators, ion conductors for electrode materials). Instead of using traditional inorganic and polymer materials, selective and effective transport can be achieved in synthesis materials by precisely designed nanochannels through rational consideration of the interfacial interactions, channel sizes, and molecular and nanoscale structural refinement. Several groups have begun to investigate water diffusion in hydrophobic carbon nanotubes.<sup>[239,244]</sup> Another material candidate to understand and optimize the fundamental transport properties could be the self-assembled nanoarrays and nanoporous.<sup>[245–247]</sup> In such tailored nanoporous materials, the surface chemistry, the pore dimension, and the molecular and nanoscale ordering can be systematically adjusted.<sup>[248,249]</sup>

In electric eels, the electrical energy is stored as sodium or potassium ions in ion channels (Figure 9).<sup>[250]</sup> The electrocytes (muscle cells that store that charge) in electrical eels are arranged in series and parallel configurations. The ions at the opposite poles of the ion channels are separated, enabling the storage of 500 V of electricity.<sup>[250]</sup> It is possible that new supercapacitors can be constructed based on similar principles. Other

natural organisms use sophisticated molecular machines, such as enzymes, to convert electrochemical energy into chemical energy (fuels) and chemicals into electricity. From a pure “battery perspective,” these catalysts are of interest because they

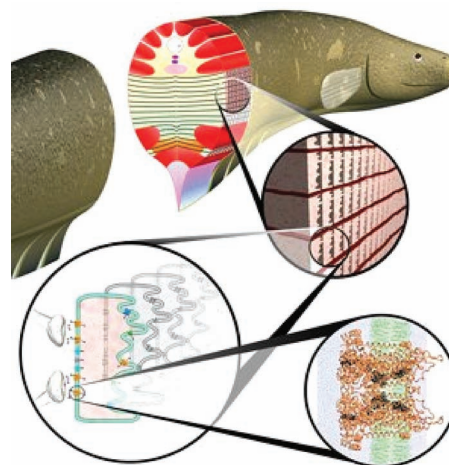


**Figure 9.** Energy storage in biological ion channels in electrical eels based on stacked membranes. Reproduced with permission.<sup>[250]</sup> Copyright 2008, Nature Publishing Group.



can participate in redox processes involving up to six electrons (in contrast to the one-electron transfer found in lithium batteries). They can also participate in reactions that either remove harmful byproducts of energy creation (e.g., converting the CO<sub>2</sub> created by burning fossil fuels into new fuels such as methanol) or create chemicals that are important components in renewable energy flows (e.g., conversion of N<sub>2</sub> into ammonia or fertilizers for biofuel production).

## Acknowledgements

The development of this manuscript and part of the research in materials synthesis and chemistry was supported by the U.S. Department of Energy (DOE), Office of Basic Energy Sciences, Division of Materials Sciences and Engineering, under Award KC020105-FWP12152. The redox flow battery research was supported by the Office of Electricity Delivery and Energy Reliability (OE) of the Department of Energy. The planar Na battery research was supported by the APAR-E of the Department of Energy. The TEM study was conducted in the William R. Wiley Environmental Molecular Sciences Laboratory (EMSL), a national scientific user facility sponsored by DOE's Office of Biological and Environmental Research and located at PNNL. PNNL is operated for DOE by Battelle under Contract DE-AC05-76RL01830.

Received: March 13, 2012

Revised: April 10, 2012

Published online: June 4, 2012

- [1] J. Liu, G. Cao, Z. Yang, D. Wang, D. Dubois, X. Zhou, G. L. Graff, L. R. Pederson, J.-G. Zhang, *ChemSusChem* **2008**, 1, 661–661.
- [2] J. L. M. a. P. A. T. Paul Butler, *Energy Storage Opportunities Analysis Phase II Final Report A Study for the DOE Energy Storage Systems Program*, Sandia National Laboratories, Albuquerque, NM **2002**.
- [3] Z. Yang, J. Zhang, M. C. W. Kintner-Meyer, X. Lu, D. Choi, J. P. Lemmon, J. Liu, *Chem. Rev.* **2011**, 111, 3577.
- [4] J. B. Goodenough, Y. Kim, *Chem. Mater.* **2010**, 22, 587.
- [5] D. Howell, *Annual Merit Review Energy Storage R&D Overview*, Washington DC **2009**.
- [6] S. L. Candelaria, Y. Shao, W. Zhou, X. Li, J. Xiao, J.-G. Zhang, Y. Wang, J. Liu, J. Li, G. Cao, *Nano Energy* **2012**, 1, 195.
- [7] X. Ji, K. T. Lee, L. F. Nazar, *Nat. Mater.* **2009**, 8, 500.
- [8] X. Li, Y. Cao, W. Qi, L. V. Saraf, J. Xiao, Z. Nie, J. Mietek, J.-G. Zhang, B. Schwenzer, J. Liu, *J. Mater. Chem.* **2011**, 21, 16603.
- [9] L. Xiao, Y. Cao, J. Xiao, B. Schwenzer, M. H. Engelhard, L. V. Saraf, Z. Nie, G. J. Exarhos, J. Liu, *Adv. Mater.* **2012**, 24, 1176.
- [10] J. Xiao, D. Mei, X. Li, W. Xu, D. Wang, G. L. Graff, W. D. Bennett, Z. Nie, L. V. Saraf, I. A. Aksay, J. Liu, J.-G. Zhang, *Nano Lett.* **2011**, 11, 5071.
- [11] J. Xiao, D. Wang, W. Xu, D. Wang, R. E. Williford, J. Liu, J.-G. Zhang, *J. Electrochem. Soc.* **2010**, 157, A487.
- [12] J. Xiao, W. Xu, D. Wang, J.-G. Zhang, *J. Electrochem. Soc.* **2010**, 157, A294.
- [13] R. Padbury, X. Zhang, *J. Power Sources* **2011**, 196, 4436.
- [14] R. E. Williford, J.-G. Zhang, *J. Power Sources* **2009**, 194, 1164.
- [15] I. Kowaluk, J. Read, M. Salomon, *Pure Appl. Chem.* **2007**, 79, 851.
- [16] L. D. Mears, H. L. Gotschall, T. Key, H. Kamath, *Handbook of Energy Storage for Transmission and Distribution Applications*, Electrical Power Research Institute and Department of Energy, Washington, DC **2003**.
- [17] The Electricity Advisory Committee of the US Department of Energy, *Bottling Electricity: Storage as a Strategic Tool for Managing Variability and Capacity Concerns in the Modern Grid*, Washington DC **2008**.
- [18] M. Kintner-Myer, PNNL report, **2012**.
- [19] D. G. B. Lee, *Massive Electricity Storage, An AIChE White Paper*, American Institute of Chemical Engineers, New York **2008**.
- [20] M. Kintner-Meyer, *Assessment on the technical potential energy storage size for integrating 300 GW of Wind energy capacity into the US grid by 2030, Preliminary Results*, Pacific Northwest National Laboratory, Richland, WA **2010**.
- [21] B. S. Lee, D. E. Gushee, *Chem. Eng. Prog.* **2008**, 104, S29.
- [22] E. E. Paul Denholm, Brendan Kirby, Michael Milligan, *The Role of Energy Storage with Renewable Electricity Generation*, National Renewable Energy Laboratory, Golden, CO **2010**.
- [23] B. E. Conway, *J. Electrochem. Soc.* **1991**, 138, 1539.
- [24] E. Frackowiak, *Phys. Chem. Chem. Phys.* **2007**, 9, 1774.
- [25] *Energy Storage Tracker 4Q11: Planned and Deployed Energy Storage Projects by World Region, Market Segment, Technology, and Application* <http://www.pikeresearch.com/research/energy-storage-tracker-4q11> (accessed May 2012).
- [26] R. H. Richman, *Flywheel Energy Storage*, EPRI Report TR-108378, Mountain View, CA **1997**.
- [27] W. Hassenzahl, *Flywheels for Electric Energy Storage*, EPRI Report TR-108889, Oakland, CA **1999**.
- [28] B. P. Roberts, in *2008 IEEE Power Energy Soc. Gen. Meet.* 1–11, **2008**, pp. 990–991.
- [29] H. M. Zhang, Y. Zhang, Z. H. Liu, X. L. Wang, *Prog. Chem.* **2009**, 21, 2333.
- [30] J. T. Kummer, N. K. Weber, *SAE Trans.* **1968**, 476, 88.
- [31] Y. F. Y. K. Yao, J. T. Kummer, *J. Inorg. Nucl. Chem.* **1967**, 29, 2453.
- [32] J. T. Kummer, N. Weber, *SAE Trans.* **1968**, 76, 88.
- [33] R. J. Bones, D. A. Teagle, S. D. Brooker, F. L. Cullen, *J. Electrochem. Soc.* **1989**, 136, 1274.
- [34] R. C. Galloway, *J. Electrochem. Soc.* **1987**, 134, 256.
- [35] C.-H. Dustmann, *J. Power Sources* **2004**, 127, 85.
- [36] J. L. Sudworth, *J. Power Sources* **2001**, 100, 149.
- [37] R. S. J. Tilly, *Sodium-Sulfure Battery*, Chapman and Hall Limited, London **1985**.
- [38] X. C. Lu, G. G. Xia, J. P. Lemmon, Z. G. Yang, *J. Power Sources* **2010**, 195, 2431.
- [39] M. Skyllas-Kazacos, M. Rychick, R. Robins, *US Patent* **1988**, 4786567.
- [40] E. Sum, M. Rychcik, M. Skyllaskazacos, *J. Power Sources* **1985**, 16, 85.
- [41] E. Sum, M. Skyllaskazacos, *J. Power Sources* **1985**, 15, 179.
- [42] M. Bartolozzi, *J. Power Sources* **1989**, 27, 219.
- [43] C. P. de Leon, A. Frias-Ferrer, J. Gonzalez-Garcia, D. A. Szanto, F. C. Walsh, *J. Power Sources* **2006**, 160, 716.
- [44] X. Xia, H. T. Liu, Y. Liu, *J. Electrochem. Soc.* **2002**, 149, A426.
- [45] Y. H. Wen, H. M. Zhang, P. Qian, H. T. Zhou, P. Zhao, B. L. Yi, Y. S. Yang, *J. Electrochem. Soc.* **2006**, 153, A929.
- [46] F. Q. Xue, Y. L. Wang, W. H. Wang, X. D. Wang, *Electrochim. Acta* **2008**, 53, 6636.
- [47] A. Price, S. Bartley, S. Male, G. Cooley, *Power Eng. J.* **1999**, 13, 122.
- [48] D. P. Scamman, G. W. Reade, E. P. L. Roberts, *J. Power Sources* **2009**, 189, 1231.
- [49] N. E. Clark, P. Lex, *Development of Zinc/Bromine Batteries for Load-Leveling Applications: Phase 2 Final Report*, Sandia National Laboratories, Albuquerque, NM **1999**.
- [50] M. Skyllaskazacos, M. Rychcik, R. G. Robins, A. G. Fane, M. A. Green, *J. Electrochem. Soc.* **1986**, 133, 1057.
- [51] A. Burke, *J. Power Sources* **2000**, 91, 37.
- [52] F. Pico, J. M. Rojo, M. L. Sanjuan, A. Anson, A. M. Benito, M. A. Callejas, W. K. Maser, M. T. Martinez, *J. Electrochem. Soc.* **2004**, 151, A831.

- [53] E. Frackowiak, K. Metenier, V. Bertagna, F. Beguin, *Appl. Phys. Lett.* **2000**, 77, 2421.
- [54] J. P. Zheng, T. R. Jow, *J. Power Sources* **1996**, 62, 155.
- [55] J. P. Zheng, T. R. Jow, *J. Electrochem. Soc.* **1995**, 142, L6.
- [56] R. Q. Fu, Z. R. Ma, J. P. Zheng, *J. Phys. Chem. B* **2002**, 106, 3592.
- [57] Z. R. Ma, J. P. Zheng, R. Q. Fu, *Chem. Phys. Lett.* **2000**, 331, 64.
- [58] Z. A. Zhang, B. C. Yang, M. G. Deng, Y. D. Hu, *J. Inorg. Mater.* **2005**, 20, 529.
- [59] D. Choi, P. N. Kumta, *J. Electrochem. Soc.* **2006**, 153, A2298.
- [60] D. W. Choi, P. N. Kumta, *Electrochem. Solid State Lett.* **2005**, 8, A418.
- [61] T. C. Liu, W. G. Pell, B. E. Conway, S. L. Roberson, *J. Electrochem. Soc.* **1998**, 145, 1882.
- [62] D. Choi, G. E. Blomgren, P. N. Kumta, *Adv. Mater.* **2006**, 18, 1178.
- [63] M. W. Xu, D. D. Zhao, S. J. Bao, H. L. Li, *J. Solid State Electrochem.* **2007**, 11, 1101.
- [64] S. Yamazaki, K. Obata, Y. Okuhama, Y. Matsuda, M. Ishikawa, *Electrochemistry* **2007**, 75, 592.
- [65] A. L. M. Reddy, S. Ramaprabhu, *J. Phys. Chem. C* **2007**, 111, 7727.
- [66] L. Ji, Z. Lin, M. Alcoutlabi, X. Zhang, *Energy Environ. Sci.* **2011**, 4, 2682.
- [67] Z. H. Lu, D. D. MacNeil, J. R. Dahn, *Electrochem. Solid State Lett.* **2001**, 4, A200.
- [68] C. S. Johnson, N. C. Li, C. Lefief, J. T. Vaughey, M. M. Thackeray, *Chem. Mater.* **2008**, 20, 6095.
- [69] A. K. Padhi, K. S. Nanjundaswamy, J. B. Goodenough, *J. Electrochem. Soc.* **1997**, 144, 1188.
- [70] O. Toprakci, L. Ji, Z. Lin, H. A. K. Toprakci, X. Zhang, *J. Power Sources* **2011**, 196, 7692.
- [71] Z. Gong, Y. Yang, *Energy Environ. Sci.* **2011**, 4, 3223.
- [72] J. Yu, K. M. Rosso, J. Liu, *J. Phys. Chem. C* **2011**, 115, 25001.
- [73] Y. G. Wang, Y. R. Wang, E. J. Hosono, K. X. Wang, H. S. Zhou, *Angew. Chem. Int. Ed.* **2008**, 47, 7461.
- [74] D. Choi, P. N. Kumta, *J. Power Sources* **2007**, 163, 1064.
- [75] A. Yamada, Y. Kudo, K. Y. Liu, *J. Electrochem. Soc.* **2001**, 148, A747.
- [76] G. H. Li, H. Azuma, M. Tohda, *Electrochem. Solid State Lett.* **2002**, 5, A135.
- [77] D. W. Choi, D. H. Wang, I. T. Bae, J. Xiao, Z. M. Nie, W. Wang, V. V. Viswanathan, Y. J. Lee, J. G. Zhang, G. L. Graff, Z. G. Yang, J. Liu, *Nano Lett.* **2010**, 10, 2799.
- [78] C. Delacourt, L. Laffont, R. Bouchet, C. Wurm, J. B. Leriche, M. Morcrette, J. M. Tarascon, C. Masquelier, *J. Electrochem. Soc.* **2005**, 152, A913.
- [79] J. Xiao, N. A. Chernova, S. Upreti, X. Chen, Z. Li, Z. Deng, D. Choi, W. Xu, Z. Nie, G. L. Graff, J. Liu, M. S. Whittingham, J.-G. Zhang, *Phys. Chem. Chem. Phys.* **2011**, 13, 18099.
- [80] T. Drezen, N. H. Kwon, P. Bowen, I. Teerlinck, M. Isono, I. Exnar, *J. Power Sources* **2007**, 174, 949.
- [81] D. Choi, J. Xiao, Y. J. Choi, J. S. Hardy, M. Vijayakumar, M. S. Bhuvaneshwari, J. Liu, W. Xu, W. Wang, Z. Yang, G. L. Graff, J.-G. Zhang, *Energy Environ. Sci.* **2011**, 4, 4560.
- [82] K. S. Kang, Y. S. Meng, J. Breger, C. P. Grey, G. Ceder, *Science* **2006**, 311, 977.
- [83] K. Amine, H. Tukamoto, H. Yasuda, Y. Fujita, *J. Electrochem. Soc.* **1996**, 143, 1607.
- [84] Q. M. Zhong, A. Bonakdarpour, M. J. Zhang, Y. Gao, J. R. Dahn, *J. Electrochem. Soc.* **1997**, 144, 205.
- [85] B. A. Boukamp, G. C. Lesh, R. A. Huggins, *J. Electrochem. Soc.* **1981**, 128, 725.
- [86] L. Ji, X. Zhang, *Energy Environ. Sci.* **2010**, 3, 124.
- [87] H. J. Kim, M. Seo, M.-H. Park, J. Cho, *Angew. Chem. Int. Ed.* **2010**, 49, 214–2149.
- [88] C. K. Chan, H. L. Peng, G. Liu, K. McIlwrath, X. F. Zhang, R. A. Huggins, Y. Cui, *Nat. Nanotechnol.* **2008**, 3, 31.
- [89] L. F. Cui, Y. Yang, C.-M. Hsu, Y. Cui, *Nano Lett.* **2009**, 9, 3370.
- [90] N.-H. Park, M. G. Kim, J. B. Joo, K. Kim, J. Kim, S. Ahn, Y. Cui, J. Cho, *Nano Lett.* **2009**, 11, 3844.
- [91] T. Song, J. L. Xia, J.-H. Lee, D. H. Lee, M.-S. Kwon, J.-M. Choi, J. Wu, S. K. Doo, H. Chang, W. I. Park, D. S. Zang, H. S. Kim, Y. G. Huang, K.-C. Hwang, J. A. Rogers, U. Y. Park, *Nano Lett.* **2010**, 10, 1710.
- [92] G. Liu, S. D. Xun, N. Vukmirovic, X. Y. Song, P. Olalde-Velasco, H. H. Zheng, V. S. Battaglia, L. W. Wang, W. L. Yang, *Adv. Mater.* **2011**, 23, 4679.
- [93] I. Kovalenko, B. Zdyrko, A. Magasinski, B. Hertzberg, Z. Milicev, R. Burtovyy, I. Luzinov, G. Yushin, *Science* **2011**, 334, 75.
- [94] N. Yabuuchi, K. J. Shimomura, Y. Shimbe, T. Ozeki, J.-Y. Son, H. Oji, Y. Katayama, T. Miura, S. Komaba, *Adv. Energy Mater.* **2011**, 1, 759.
- [95] N.-S. Choi, K. H. Yew, K. Y. Lee, M. S. Sung, H. Kim, S.-S. Kim, *J. Power Sources* **2006**, 161, 1254.
- [96] Y.-S. Hu, R. Demir-Cakan, M.-M. Titirici, J.-O. Muller, R. Schlogl, M. Antonietti, J. Maier, *Angew. Chem. Int. Ed.* **2008**, 47, 1645.
- [97] W. Wang, M. K. Datta, P. N. Kumta, *J. Mater. Chem.* **2007**, 17, 3229.
- [98] S.-H. Ng, J. Z. Wang, D. Wexler, K. Konstantinov, Z.-P. Guo, H.-K. Liu, *Angew. Chem. Int. Ed.* **2006**, 45, 6896.
- [99] W. C. Zhou, S. Upreti, M. S. Whittingham, *Electrochem. Commun.* **2011**, 13, 1102.
- [100] J. Xiao, W. Xu, D. Y. Wang, D. W. Choi, W. Wang, X. L. Li, G. L. Graff, J. Liu, J.-G. Zhang, *J. Electrochem. Soc.* **2010**, 157, A1047.
- [101] W. Wang, P. N. Kumta, *ACS Nano* **2010**, 4, 2233.
- [102] J. C. Guo, C. S. Wang, *Chem. Commun.* **2010**, 46, 1428.
- [103] J. K. Lee, K. B. Smith, C. M. Hayner, H. H. Kung, *Chem. Commun.* **2010**, 46, 2025.
- [104] X. Zhao, C. M. Hayner, M. C. Kung, H. H. Kung, *Adv. Energy Mater.* **2011**, 1, 1079.
- [105] K. Evanoff, A. Magasinski, J. B. Yang, G. Yushin, *Adv. Energy Mater.* **2011**, 1, 495.
- [106] S. C. Zhang, Z. J. Du, R. X. Lin, T. Jiang, G. R. Liu, X. M. Wu, D. S. Weng, *Adv. Mater.* **2010**, 22, 5378.
- [107] X. L. Chen, K. Gerasopoulos, J. C. Guo, A. Brown, C. S. Wang, R. Ghodssi, J. N. Culver, *ACS Nano* **2010**, 4, 5366.
- [108] X. L. Chen, K. Gerasopoulos, J. C. Guo, A. Brown, C. S. Wang, R. Ghodssi, J. N. Culver, *Adv. Funct. Mater.* **2011**, 21, 380.
- [109] Y. Yu, L. Gu, C. B. Zhu, S. Tsukimoto, P. A. van Aken, J. Maier, *Adv. Mater.* **2010**, 22, 2247.
- [110] H. J. Kim, B. H. Han, J. B. Choo, J. Cho, *Angew. Chem. Int. Ed.* **2008**, 47, 10151.
- [111] A. Magasinski, P. Dixon, B. Hertzberg, A. Kvit, J. Ayala, G. Yushin, *Nat. Mater.* **2010**, 9, 353.
- [112] B. Hertzberg, A. Alexeev, G. Yushin, *J. Am. Chem. Soc.* **2010**, 132, 8548.
- [113] J. C. Guo, A. Sun, C. S. Wang, *Electrochem. Commun.* **2010**, 12, 981.
- [114] Y. Yao, M. T. McDowell, I. Ryu, H. Wu, N. Liu, L. B. Hu, W. D. Nix, Y. Cui, *Nano Lett.* **2011**, 11, 2949.
- [115] L. Ji, K.-H. Jung, A. J. Medford, X. Zhang, *J. Mater. Chem.* **2009**, 19, 4992.
- [116] L. Ji, H. Zheng, A. Ismach, Z. Tan, S. Xun, E. Lin, V. Battaglia, V. Srinivasan, Y. Zhang, *Nano Energy* **2012**, 1, 164.
- [117] S. W. Lee, M. T. McDowell, J. W. Choi, Y. Cui, *Nano Lett.* **2011**, 11, 3034.
- [118] H. Ghassemi, M. Au, N. Chen, P. A. Heiden, R. S. Yassar, *ACS Nano* **2011**, 5, 7805.
- [119] X. H. Liu, L. Q. Zhang, L. Zhong, Y. Liu, H. Zheng, J. W. Wang, J. H. Cho, S. A. Dayeh, S. T. Picraux, J. P. Sullivan, S. X. Mao, Z. Z. Ye, J. Y. Huang, *Nano Lett.* **2011**, 11, 2251.
- [120] J. Li, J. R. Dahn, *J. Electrochem. Soc.* **2007**, 154, A156.

- [121] M. N. Obrovac, L. Christensen, *Electrochem. Solid State Lett.* **2004**, *7*, A93.
- [122] Z. G. Wang, W. Xu, J. Liu, F. Gao, L. Kovarik, J. G. Zhang, J. Howe, D. J. Burton, Z. Y. Liu, X. C. Xiao, S. Thevuthasan, D. R. Baer, *Nano Lett.* **2012**, *12*, 1624.
- [123] X. Huang, *J. Solid State Electrochem.* **2011**, *15*, 649.
- [124] M. L. Sushko, K. M. Rosso, J.-G. Zhang, J. Liu, *J. Phys. Chem. Lett.* **2011**, *2*, 2352.
- [125] B. Schwenzer, J. Zhang, S. Kim, L. Li, J. Liu, Z. Yang, *ChemSusChem* **2011**, *4*, 1388.
- [126] B. Schwenzer, S. Kim, M. Vijayakumar, Z. Yang, J. Liu, *J. Membr. Sci.* **2011**, *372*, 11.
- [127] Q. Luo, H. Zhang, J. Chen, D. You, C. Sun, Y. Zhang, *J. Membr. Sci.* **2008**, *325*, 553.
- [128] S. Kim, J. Yan, B. Schwenzer, J. Zhang, L. Li, J. Liu, Z. Yang, M. A. Hickner, *Electrochem. Commun.* **2010**, *12*, 1650.
- [129] Z. Wen, J. Cao, Z. Gu, X. Xu, F. Zhang, Z. Lin, *Solid State Ionics* **2008**, *179*, 1697.
- [130] J. Hassoun, B. Scrosati, *Adv. Mater.* **2010**, *22*, 5198.
- [131] G. Girishkumar, B. McCloskey, A. C. Luntz, S. Swanson, W. Wilcke, *J. Phys. Chem. Lett.* **2010**, *1*, 2193.
- [132] S. J. Paddison, *First principles modeling of sulfonic acid based ionomer membranes*. John Wiley and Sons, Chichester, UK **2003**, Vol. 3.
- [133] S. J. Paddison, *Annu. Rev. Mater. Res.* **2003**, *33*, 289.
- [134] K. Schmidt-Rohr, Q. Chen, *Nat. Mater.* **2008**, *7*, 75.
- [135] K. D. Kreuer, *J. Membr. Sci.* **2001**, *185*, 29.
- [136] W. H. J. Hogarth, J. C. D. da Costa, G. Q. Lu, *J. Power Sources* **2005**, *142*, 223.
- [137] K. D. Kreuer, *Solid State Ionics* **1997**, *97*, 1.
- [138] K. D. Kreuer, *Solid State Ionics* **2000**, *136*, 149.
- [139] J. Zeng, C. P. Jiang, Y. H. Wang, J. W. Chen, S. F. Zhu, B. J. Zhao, R. Wang, *Electrochem. Commun.* **2008**, *10*, 372.
- [140] J. Xi, Z. Wu, X. Qiu, L. Chen, *J. Power Sources* **2007**, *166*, 531.
- [141] Q. T. Luo, H. M. Zhang, J. Chen, D. J. You, C. X. Sun, Y. Zhang, *J. Membr. Sci.* **2008**, *325*, 553.
- [142] B. Schwenzer, S. Kim, M. Vijayakumar, Z. G. Yang, J. Liu, *J. Membr. Sci.* **2011**, *372*, 11.
- [143] M. Vijayakumar, M. S. Bhuvaneswari, P. Nachimuthu, B. Schwenzer, S. Kim, Z. G. Yang, J. Liu, G. L. Graff, S. Thevuthasan, J. Z. Hu, *J. Membr. Sci.* **2011**, *366*, 325.
- [144] L. Ji, M. Rao, H. Zheng, L. Zhang, Y. Li, W. Duan, J. Guo, E. J. Cairns, Y. Zhang, *J. Am. Chem. Soc.* **2011**, *133*, 18522.
- [145] L. Ji, M. Rao, S. Aloni, L. Wang, E. J. Cairns, Y. Zhang, *Energy Environ. Sci.* **2011**, *4*, 5053.
- [146] W. Skyllas-Kazacos, C. Menictas, M. Kazacos, *J. Electrochem. Soc.* **1996**, *143*, L86.
- [147] M. Skyllas-Kazacos, *J. Power Sources* **2003**, *124*, 299.
- [148] M. Skyllas-Kazacos, C. Peng, M. Cheng, *Electrochem. Solid State Lett.* **1999**, *2*, 121.
- [149] L. Y. Li, S. Kim, W. Wang, M. Vijayakumar, Z. M. Nie, B. W. Chen, J. L. Zhang, G. G. Xia, J. Z. Hu, G. Graff, J. Liu, Z. G. Yang, *Adv. Energy Mater.* **2011**, *1*, 394.
- [150] C. F. Baes Jr, R. E. Mesmer, *The Hydrolysis of Cations*, Robert E Krieger Publishing Company, Malabar, FL **1986**.
- [151] M. Vijayakumar, S. D. Burton, C. Huang, L. Li, Z. Yang, G. L. Graff, J. Liu, J. Z. Hu, M. Skyllas-Kazacos, *J. Power Sources* **2010**, *195*, 7709.
- [152] C. Madic, G. M. Begun, D. E. Hobart, R. L. Hahn, *Inorg. Chem.* **1984**, *23*, 1914.
- [153] N. Kausar, R. Howe, M. Skyllas-Kazacos, *J. Appl. Electrochem.* **2001**, *31*, 1327.
- [154] G. A. Pozarnsky, A. V. McCormick, *Chem. Mater.* **1994**, *6*, 380.
- [155] G. A. Pozarnsky, A. V. McCormick, *J. Mater. Chem.* **1994**, *4*, 1749.
- [156] L. T. Lam, R. Louey, *J. Power Sources* **2006**, *158*, 1140.
- [157] P. T. Moseley, R. F. Nelson, A. F. Hollenkamp, *J. Power Sources* **2006**, *157*, 3.
- [158] P. T. Moseley, *J. Power Sources* **2009**, *191*, 134.
- [159] D. Pavlov, T. Rogachev, P. Nikolov, G. Petkova, *J. Power Sources* **2009**, *191*, 58.
- [160] B. Scrosati, J. Garche, *J. Power Sources* **2010**, *195*, 2419.
- [161] Z. G. Yang, D. Choi, S. Kerisit, K. M. Rosso, D. H. Wang, J. Zhang, G. Graff, J. Liu, *J. Power Sources* **2009**, *192*, 588.
- [162] D. Wang, R. Kou, D. Choi, Z. Yang, Z. Nie, J. Li, L. V. Saraf, D. Hu, J. Zhang, G. L. Graff, J. Liu, M. A. Pope, I. A. Aksay, *ACS Nano* **2010**, *4*, 1587.
- [163] D. Wang, D. Choi, Z. Yang, V. V. Viswanathan, Z. Nie, C. Wang, Y. Song, J.-G. Zhang, J. Liu, *Chem. Mater.* **2008**, *20*, 3435.
- [164] L. Ji, Z. Tan, T. R. Kuykendall, S. Aloni, S. Xun, E. Lin, V. Battaglia, Y. Zhang, *Phys. Chem. Chem. Phys.* **2011**, *13*, 7170.
- [165] Z. Chen, M. Zhou, Y. Cao, X. Ai, H. Yang, J. Liu, *Adv. Energy Mater.* **2012**, *2*, 95.
- [166] J. Xiao, X. Wang, X.-Q. Yang, S. Xun, G. Liu, P. K. Koech, J. Liu, J. P. Lemmon, *Adv. Funct. Mater.* **2011**, *21*, 2840.
- [167] Z. H. Li, D. M. Zhang, F. X. Yang, *J. Mater. Sci.* **2009**, *44*, 2435.
- [168] D. W. Choi, D. H. Wang, V. V. Viswanathan, I. T. Bae, W. Wang, Z. M. Nie, J. G. Zhang, G. L. Graff, J. Liu, Z. G. Yang, T. Duong, *Electrochem. Commun.* **2010**, *12*, 378.
- [169] D. H. Wang, D. W. Choi, J. Li, Z. G. Yang, Z. M. Nie, R. Kou, D. H. Hu, C. M. Wang, L. V. Saraf, J. G. Zhang, I. A. Aksay, J. Liu, *ACS Nano* **2009**, *3*, 907.
- [170] S. H. Kang, V. G. Pol, I. Belharouak, M. M. Thackeray, *J. Electrochem. Soc.* **2010**, *157*, A267.
- [171] R. E. Williford, V. V. Viswanathan, J. G. Zhang, *J. Power Sources* **2009**, *189*, 101.
- [172] V. V. Viswanathan, D. Choi, D. H. Wang, W. Xu, S. Towne, R. E. Williford, J. G. Zhang, J. Liu, Z. G. Yang, *J. Power Sources* **2010**, *195*, 3720.
- [173] T. Oshima, M. Kajita, A. Okuno, *Int. J. Appl. Ceramic Technol.* **2004**, *1*, 269.
- [174] I. O. K. Hagman, P. Kierkegaard, *Acta Chem. Scand.* **1968**, *22*, 1822.
- [175] J. P. Lemmon, Z. G. Yang, X. C. Lu, G. G. Xia, V. Sprenkle, K. Meinhardt, J. Liu, *The 217th Electrochemical Society Meeting, Vancouver Canada*, **2010**, Abstract 371.
- [176] X. C. Lu, G. G. Xia, K. Meinhardt, J. P. Lemmon, V. Sprenkle, Z. G. Yang, *TMS2010, Seattle WA*, **2010**.
- [177] R. D. Rauh, K. M. Abraham, G. F. Pearson, J. K. Surprenant, S. B. Brummer, *J. Electrochem. Soc.* **1979**, *126*, 523.
- [178] X. L. Ji, K. T. Lee, L. F. Nazar, *Nat. Mater.* **2009**, *8*, 500.
- [179] S. E. Cheon, K. S. Ko, J. H. Cho, S. W. Kim, E. Y. Chin, H. T. Kim, *J. Electrochem. Soc.* **2003**, *150*, A800.
- [180] Y. V. Mikhaylik, J. R. Akridge, *J. Electrochem. Soc.* **2004**, *151*, A1969.
- [181] L. X. Yuan, J. K. Feng, X. P. Ai, Y. L. Cao, S. L. Chen, H. X. Yang, *Electrochem. Commun.* **2006**, *8*, 610.
- [182] J. H. Shin, E. J. Cairns, *J. Power Sources* **2008**, *177*, 537.
- [183] J. Wang, S. Y. Chew, Z. W. Zhao, S. Ashraf, D. Wexler, J. Chen, S. H. Ng, S. L. Chou, H. K. Liu, *Carbon* **2008**, *46*, 229.
- [184] B. Zhang, X. Qin, G. R. Li, X. P. Gao, *Energy Environ. Sci.* **2010**, *3*, 1531.
- [185] C. Lai, X. P. Gao, B. Zhang, T. Y. Yan, Z. Zhou, *J. Phys. Chem. C* **2009**, *113*, 4712.
- [186] X. L. Ji, L. F. Nazar, *J. Mater. Chem.* **2010**, *20*, 9821.
- [187] C. D. Liang, N. J. Dudney, J. Y. Howe, *Chem. Mater.* **2009**, *21*, 4724.
- [188] Y. L. Cao, X. L. Li, I. A. Aksay, J. Lemmon, Z. M. Nie, Z. G. Yang, J. Liu, *Phys. Chem. Chem. Phys.* **2011**, *13*, 7660.
- [189] N. Jayaprakash, J. Shen, S. S. Moganty, A. Corona, L. A. Archer, *Angew. Chem. Int. Ed.* **2011**, *50*, 5904.
- [190] S.-R. Chen, Y.-P. Zhai, G.-L. Xu, Y.-X. Jiang, D.-Y. Zhao, J.-T. Li, L. Huang, S.-G. Sun, *Electrochim. Acta* **2011**, *56*, 9549.



- [191] H. L. Wang, Y. Yang, Y. Y. Liang, J. T. Robinson, Y. G. Li, A. Jackson, Y. Cui, H. J. Dai, *Nano Lett.* **2011**, *11*, 2644.
- [192] F. Wu, S. X. Wu, R. J. Chen, J. Z. Chen, S. Chen, *Electrochem. Solid State Lett.* **2010**, *13*, A29.
- [193] F. Wu, J. Z. Chen, R. J. Chen, S. X. Wu, L. Li, S. Chen, T. Zhao, *J. Phys. Chem. C* **2011**, *115*, 6057.
- [194] J. Wang, J. Chen, K. Konstantinov, L. Zhao, S. H. Ng, G. X. Wang, Z. P. Guo, H. K. Liu, *Electrochim. Acta* **2006**, *51*, 4634.
- [195] M. M. Sun, S. C. Zhang, T. Jiang, L. Zhang, J. H. Yu, *Electrochem. Commun.* **2008**, *10*, 1819.
- [196] L. L. Qiu, S. C. Zhang, L. Zhang, M. M. Sun, W. K. Wang, *Electrochim. Acta* **2010**, *55*, 4632.
- [197] X. G. Yu, J. Y. Xie, J. Yang, H. J. Huang, K. Wang, Z. S. Wen, *J. Electroanal. Chem.* **2004**, *573*, 121.
- [198] J. L. Wang, J. Yang, J. Y. Xie, N. X. Xu, *Adv. Mater.* **2002**, *14*, 963.
- [199] J. L. Wang, J. Yang, C. R. Wan, K. Du, J. Y. Xie, N. X. Xu, *Adv. Funct. Mater.* **2003**, *13*, 487.
- [200] X. U. Yu, J. Y. Xie, Y. Li, H. J. Huang, C. Y. Lai, K. Wang, *J. Power Sources* **2005**, *146*, 335.
- [201] S. Visco, *4th Symp. Energy Storage: Beyond Lithium Ion*, Richland, WA, USA, July 8, **2011**.
- [202] T. Zhang, N. Imanishi, S. Hasegawa, A. Hirano, J. Xie, Y. Takeda, O. Yamamoto, N. Sammes, *J. Electrochem. Soc.* **2008**, *155*, A965.
- [203] Y. Shimonishi, T. Zhang, N. Imanishi, D. Im, D. J. Lee, A. Hirano, Y. Takeda, O. Yamamoto, N. Sammes, *J. Power Sources* **2011**, *196*, 5128.
- [204] Y. G. Wang, H. S. Zhou, *J. Power Sources* **2010**, *195*, 358.
- [205] E. Yoo, H. S. Zhou, *ACS Nano* **2011**, *5*, 3020.
- [206] H. S. Zhou, Y. G. Wang, H. Q. Li, P. He, *ChemSusChem* **2010**, *3*, 1009.
- [207] K. M. Abraham, Z. Jiang, *J. Electrochem. Soc.* **1996**, *143*, 1.
- [208] A. Kraytsberg, Y. Ein-Eli, *J. Power Sources* **2011**, *196*, 886.
- [209] G. Girishkumar, B. McCloskey, A. C. Luntz, S. Swanson, W. Wilcke, *J. Phys. Chem. Lett.* **2010**, *1*, 2193.
- [210] R. Padbury, X. W. Zhang, *J. Power Sources* **2011**, *196*, 4436.
- [211] M. K. Song, S. J. Park, F. M. Alamgir, J. Cho, M. L. Liu, *Mater. Sci. Eng. R* **2011**, *72*, 203.
- [212] P. G. Bruce, L. J. Hardwick, K. M. Abraham, *MRS Bull.* **2011**, *36*, 506.
- [213] P. G. Bruce, S. A. Freunberger, L. J. Hardwick, J. M. Tarascon, *Nat. Mater.* **2012**, *11*, 19.
- [214] J. Christensen, P. Albertus, R. S. Sanchez-Carrera, T. Lohmann, B. Kozinsky, R. Liedtke, J. Ahmed, A. Kojic, *J. Electrochem. Soc.* **2012**, *159*, R1.
- [215] K. Brandt, *Solid State Ionics* **1994**, *69*, 173.
- [216] S. A. Freunberger, Y. H. Chen, N. E. Drewett, L. J. Hardwick, F. Barde, P. G. Bruce, *Angew. Chem. Int. Ed.* **2011**, *50*, 8609.
- [217] Y. Y. Shao, W. Xu, F. Ding, J. G. Zhang, Y. Wang, J. Liu, *4th Symp. Energy Storage: Beyond Lithium Ion*, Richland, WA, USA **2011**.
- [218] S. A. Freunberger, Y. H. Chen, Z. Q. Peng, J. M. Griffin, L. J. Hardwick, F. Barde, P. Novak, P. G. Bruce, *J. Am. Chem. Soc.* **2011**, *133*, 8040.
- [219] J. Barker, M. Y. Saidi, J. L. Swoyer, *Electrochem. Solid-State Lett.* **2003**, *6*, A1.
- [220] Y. Cao, L. Xiao, W. Wang, D. Choi, Z. Nie, J. Yu, L. V. Saraf, Z. Yang, J. Liu, *Adv. Mater.* **2011**, *23*, 3155.
- [221] D. Kim, S.-H. Kang, M. Slater, S. Rood, J. T. Vaughey, N. Karan, M. Balasubramanian, C. S. Johnson, *Adv. Energy Mater.* **2011**, *1*, 333.
- [222] H. Liu, H. Zhou, L. Chen, Z. Tang, W. Yang, *J. Power Sources* **2011**, *196*, 814.
- [223] J. F. Whitacre, A. Tevar, S. Sharma, *Electrochem. Commun.* **2010**, *12*, 463.
- [224] D. A. Stevens, J. R. Dahn, *J. Electrochem. Soc.* **2000**, *147*, 1271.
- [225] M. Dubois, D. Billaud, *J. Solid State Chem.* **1996**, *127*, 123.
- [226] M. M. Doeff, Y. Ma, S. J. Visco, L. C. D. Jonghe, *J. Electrochem. Soc.* **1993**, *140*, L169.
- [227] R. Alcántara, J. M. Jiménez-Mateos, P. Lavela, J. L. Tirado, *Electrochem. Commun.* **2001**, *3*, 639.
- [228] R. Alcántara, P. Lavela, G. F. Ortiz, J. L. Tirado, *Electrochem. Solid-State Lett.* **2005**, *8*, A222.
- [229] S. Wenzel, T. Hara, J. Janek, P. Adelhelm, *Energy Environ. Sci.* **2011**, *4*, 3342.
- [230] X. Xia, M. N. Obrovac, J. R. Dahn, *Electrochem. Solid-State Lett.* **2011**, *14*, A130.
- [231] S. Yang, P. Y. Zavalij, M. S. Whittingham, *Electrochem. Commun.* **2003**, *5*, 587.
- [232] N. L. Rock, P. N. Kumta, *J. Power Sources* **2007**, *164*, 829.
- [233] Z. Chen, Y. Cao, J. Qian, X. Ai, H. Yang, *J. Mater. Chem.* **2010**, *20*, 7266.
- [234] Z. Chen, Y. Cao, J. Qian, X. Ai, H. Yang, *J. Phys. Chem. C* **2010**, *114*, 15196.
- [235] L. Ji, Z. Tan, T. Kuykendall, E. J. An, Y. Fu, V. Battaglia, Y. Zhang, *Energy Environ. Sci.* **2011**, *4*, 3611.
- [236] H. Baker, H. Okamoto, *Alloy Phase Diagrams 2nd ed. Vol. 3*, ASM International, Materials Park, OH **1992**, pp. 3361.
- [237] L. Xiao, Y. Cao, J. Xiao, W. Wang, L. Kovarik, Z. Nie, J. Liu, *Chem. Commun.* **2012**, *48*, 3321.
- [238] C. D. Wessells, R. A. Huggins, Y. Cui, *Nat. Commun.* **2011**, *2*, 550.
- [239] G. Hummer, *Mol. Phys.* **2007**, *105*, 201.
- [240] G. M. Preston, T. P. Carroll, W. B. Guggino, P. Agre, *Science* **1992**, *256*, 385.
- [241] R. Pomes, B. Roux, *Biophys. J.* **1996**, *71*, 19.
- [242] R. Pomes, B. Roux, *Biophys. J.* **1998**, *75*, 33.
- [243] D. A. Doyle, J. M. Cabral, R. A. Pfuetzner, A. L. Kuo, J. M. Gulbis, S. L. Cohen, B. T. Chait, R. MacKinnon, *Science* **1998**, *280*, 69.
- [244] D. Nepal, K. E. Geckeler, *Small* **2007**, *3*, 1259.
- [245] J. S. Beck, J. C. Vartuli, W. J. Roth, M. E. Leonowicz, C. T. Kresge, K. D. Schmitt, C. T. W. Chu, D. H. Olson, E. W. Sheppard, S. B. McCullen, J. B. Higgins, J. L. Schlenker, *J. Am. Chem. Soc.* **1992**, *114*, 10834.
- [246] C. T. Kresge, M. E. Leonowicz, W. J. Roth, J. C. Vartuli, J. S. Beck, *Nature* **1992**, *359*, 710.
- [247] D. Y. Zhao, J. L. Feng, Q. S. Huo, N. Melosh, G. H. Fredrickson, B. F. Chmelka, G. D. Stucky, *Science* **1998**, *279*, 548.
- [248] X. Feng, G. E. Fryxell, L. Q. Wang, A. Y. Kim, J. Liu, K. M. Kemner, *Science* **1997**, *276*, 923.
- [249] Y. S. Shin, J. Liu, L. Q. Wang, Z. M. Nie, W. D. Samuels, G. E. Fryxell, G. J. Exarhos, *Angew. Chem. Int. Ed.* **2000**, *39*, 2702.
- [250] J. Xu, D. A. Lavan, *Nat. Nanotechnol.* **2008**, *3*, 666.
- [251] Y. Y. Shao, F. Ding, J. Xiao, J. Zhang, W. Xu, S. K. Park, J. G. Zhang, Y. Wang, J. Liu, *Adv. Funct. Mater.* DOI: 10.1002/adfm.201200688.
- [252] X. C. Lu, G. Coffey, K. Meinhardt, V. Sprenkle, Z. G. Yang, J. Lemmon, *ECS Trans.* **2010**, *28*, 7.
- [253] Z. G. Yang, J. Liu, S. Baskaran, C. H. Imhoff, J. D. Holladay, *JOM* **2010**, *62*, 14.